European Journal of Medicinal Chemistry 179 (2019) 56–77

Contents lists available at ScienceDirect

European Journal of Medicinal Chemistry

journal homepage: http://www.elsevier.com/locate/ejmech

Review article

Biomedical applications of radioiodinated peptides

Maria Cristina Oliveira*, João D.G. Correia**

Centro de Ciências e Tecnologias Nucleares, Departamento de Engenharia e Ciências Nucleares, Instituto Superior Técnico, Universidade de Lisboa, CTN, Estrada Nacional 10 (km 139,7), 2695-066, Bobadela LRS, Portugal

ARTICLE INFO

Article history:
Received 15 April 2019
Received in revised form
4 June 2019
Accepted 4 June 2019
Available online 7 June 2019

Keywords:
Biomedical applications
Molecular imaging
Peptides
Radioiodine
Radionuclide therapy

ABSTRACT

The overexpression of peptide receptors in certain tumors as compared to endogeneous expression levels represents the molecular basis for the design of peptide-based tools for targeted nuclear imaging and therapy. Receptor targeting with radiolabelled peptides became a very important imaging and/or therapeutic approach in nuclear medicine and oncology. A great variety of peptides has been radiolabelled with clinical relevant radionuclides, such as radiometals and radiohalogens. However, to the best of our knowledge concise and updated reviews providing information about the biomedical application of radioiodinated peptides are still missing. This review outlines the synthetic efforts in the preparation of radioiodinated peptides highlighting the importance of radioiodine in nuclear medicine, giving an overview of the most relevant radioiodination strategies that have been employed and describes relevant examples of their use in the biomedical field.

Contents

1. Introduction

Naturally occurring peptides play a key role in all living systems and are responsible for a variety of essential functions. Stable derivatives of those peptides or newly engineered peptide sequences have emerged as important tools for biomedical applications. Indeed, they are being exploited in tissue engineering, wound

* Corresponding author.
** Corresponding author.
E-mail addresses: cristinaoliveira@ctn.tecnico.ulisboa.pt (M.C. Oliveira), jgalamba@ctn.tecnico.ulisboa.pt (J.D.G. Correia).

https://doi.org/10.1016/j.ejmech.2019.06.014
0223-5234/

healing, and regenerative medicine; as cell penetrating-peptides for transporting drugs and/or nanoplatforms across cell membranes; as antimicrobial agents; as target-specific drugs; and as unique tools for radionuclide therapy and/or molecular imaging in nuclear medicine, just to mention a few representative examples [1–4]. Radiopeptides are well established target-specific radiopharmaceuticals in nuclear medicine, with recognized importance in cancer imaging and peptide receptor radionuclide therapy (PRRT) due to the fact that human cancers often overexpress specific peptide receptors. The most paradigmatic and successful examples have been the use of radiolabeled somatostatin derivatives for single photon emission computed tomography (SPECT, γ-emitting radionuclides) and positron emission tomography (PET, β^+-emitting radionuclides), and for treatment (β^--emitting radionuclides) of somatostatin receptor type 2 (sstr2) positive tumors, namely neuroendocrine tumors. The great majority of the radiopeptides used are based on radiometals such as ^{99m}Tc, ^{68}Ga, and ^{111}In for imaging or based on ^{177}Lu and ^{90}Y for systemic therapy, which explains the excellent reviews covering a broad range of topics related to radiopetides and their clinical applications in cancer SPECT- or PET-imaging and PRRT in recent years [5–8]. On the contrary, as far as the authors are aware, little attention has been paid to radioiodinated peptides and their biomedical applications.

Brought together the importance of radioiodine in nuclear medicine, discussed below, the recent success of radioiodinated antibody-based drugs in the clinical set (*e.g.* [^{131}I]tositumomab for the treatment of CD20-positive non-Hodgkin's lymphoma) and, to the best of our knowledge, the lack of reviews providing a compact and up-to-date summary of radioiodinated bioactive peptides and their biomedical applications, prompted us to look deeper into this topic, mainly from a (radio)chemist perspective. Herein, we will firstly refer to the importance of radioiodine in nuclear medicine, and present the most relevant radioiodination strategies and purification methods applied to radiopeptides. Then, an overview of the most thoroughly explored radioiodinated peptide families will be given. The chemistry, radiochemistry and, when relevant, the biological behaviour of radioiodinated receptor-binding peptides explored for nuclear imaging or PRRT in the last decades will be reviewed.

1.1. Radioisotopes of iodine

The radioisotopes of iodine with relevant biomedical applications, namely in nuclear medicine and radiopharmaceutical chemistry, are described in Table 1.

Radioisotopes of iodine present a unique combination of convenient nuclear properties, high specific activity and versatile chemistry. Moreover, radioiodine represents the first example of a theranostic agent as it permits both diagnosis and therapy, depending on the emission characteristics of the selected radioisotope. That is the case of ^{131}I, which is simultaneously a γ- and a β^--emitter, and used for diagnosis and therapy. Indeed, radioiodine theranostics ([^{131}I]NaI) has been extensively applied for the management of differentiated thyroid cancer since the 1950s [10–13].

Moreover, due to their physical and chemical characteristics, and availability,^{123}I, ^{125}I and ^{131}I have been widely used, especially in the labeling of monoclonal antibodies, peptides or other small molecules (*e.g.* estradiol derivatives), for diagnostic and therapeutic applications in nuclear medicine [14–18]. The positron emitter ^{124}I is being envisaged as a promising radiotracer for PET imaging due its adequate nuclear properties, namely the favourable 4.2 days half-life, together with the ease of production on cyclotrons [19–22]. Its long half-life is particularly attractive for imaging purposes using conventional immunoglobulin G (IgG) molecules or their conjugates as target-specific moieties.

Both ^{125}I and ^{131}I are reactor-produced and therefore less expensive and more readily available than the cyclotron-produced radioisotope ^{123}I. Yet, the latter is the most appropriate for *in vivo* imaging due to its convenient half-life (13.2 h) and emitted photon energy of 159 keV. ^{125}I with its long half-life of 60 days and the low energy of the emitted photons (27–35 keV) is the most commonly used for *in vitro* biological assays and preclinical studies. The ^{131}I isotope presents an half-life of 8 days and an emitted radiation of both 364 keV photons and low energy β^- particles, suitable for scintigraphic applications and for radionuclide therapy, respectively [23]. Indeed, this radioisotope is routinely used in the clinical setting for the management of thyroid cancer.

1.2. Radioiodination methods

Although the simple inorganic salts [$^{123/131}$I]NaI are radiopharmaceuticals *per se*, being directly administered to patients for imaging or treating thyroid cancer, target-specific radioiodinated organic molecules need to be previously radioiodinated. Several radiochemical methods for the labelling of biomolecules or small molecules with iodine radioisotopes are available [14–18]. The main radioiodination strategies involve either *direct labeling* via electrophilic substitution at reactive moieties, such as an aromatic amino acid, or *indirect labeling* via prosthetic groups. Isotopic exchange can also be applied when an iodine atom is already present in the precursor [24]. However, this approach leads to radioiodinated molecules with low specific activity [14].

Direct labeling is usually performed by *direct radioiodination* of tyrosine (Tyr) or histidine (His) residues already present in the amino acid chain, in the case of peptides or antibodies. To allow direct iodination many peptide analogues have also been prepared by replacing an existing phenylamine (Phe) with Tyr or by adding Tyr to sequence sites that are not critical for biological activity or receptor binding. For the sake of illustrative example, let us refer to the case of octreotide (Fig. 1), a somatostatin analogue that cannot

Table 1
Nuclear properties and application of some iodine radionuclides [9].

	^{123}I	^{124}I	^{125}I	^{131}I
Production	Cyclotron	Cyclotron	Nuclear reactor	Nuclear reactor
Decay mode	Electron capture	Electron capture β+ decay	Electron capture	β^- decay
Physical half life	13.22 h	4.18 days	59.39 days	8.02 days
γ energy[a] (keV)	159 (83%)	511 (annihilation)	35.5 (7%)	364 (81%)
β energy[a] (keV)		2140		606
Auger electron emission	28.4 electron/decay		19.5 electron/decay	
Application	SPECT imaging Targeted radiotherapy	PET imaging	In vitro bioassays Micro SPECT Targeted radiotherapy	SPECT imaging Radiotherapy

[a] Only primary emissions have been considered.

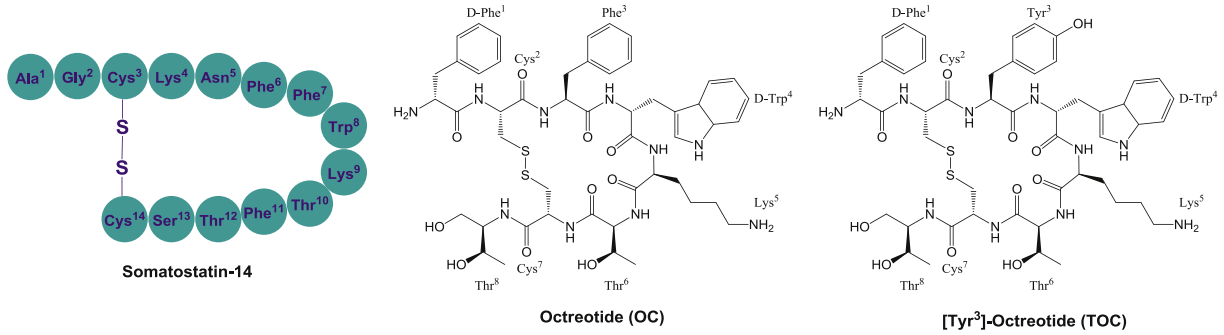

Fig. 1. Somatostatin-14 and the derivatives octreotide (OC) and Tyr [3]-octreotide (TOC).

be easily radioiodinated. Indeed, a synthetic analogue ([Tyr^3]-octreotide, TOC), in which 3-Phe was replaced by 3-Tyr, has been designed in order to allow its easier radioiodination while preserving biological activity and has been successfully used in somatostatin receptor studies *in vitro* [25] and scintigraphic visualization of neuroendocrine tumors [26–28].

In the "traditional" direct labeling approach radioiodination is carried out by "radioiodo-deprotonation", which involves the substitution of a Tyr or His aromatic proton by the electrophilic radioiodine (I^+), usually generated *in situ* by oxidation of radioiodide, available as basic or neutral aqueous solutions, with an oxidizing agent (Fig. 2) [15,29–31].

Under optimized conditions, a spontaneous electrophilic substitution occurs on aromatic rings as depicted in Fig. 3.

Tyrosine is generally preferred over histidine for labeling because of the milder reaction conditions needed for iodination and its stability towards non-enzymatic deiodination. Also, the radiochemical yield of tyrosine radioiodination is usually higher.

Tyrosine moieties are usually labelled at pH values around 7.5 whereas radioiodination of histidine residues is carried out at higher pH values ($\approx$8.5) [32,33]. Ghrelin, the endogenous ligand for the growth hormone secretagogue receptors (GHS-R), was radioiodinated on His [9] using the classical chloramine T method [34,35].

Although chloramine-T has demonstrated to be a very effective radioiodination agent (Fig. 2), and several peptides have been radiolabelled by the chloramine-T method, various by-products can arise from side-reactions, especially in the case of peptides or proteins, demanding additional purification steps for their separation [14]. The use of immobilized chloramine-T on polystyrene beads (Iodobeads) allows for easy separation of the oxidizing agent from the reaction mixture avoiding the use of a reducing agent.

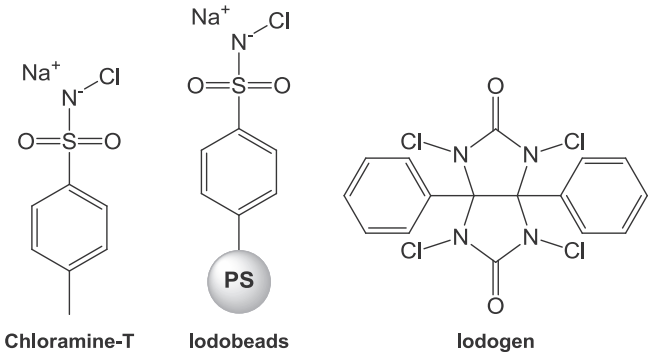

Fig. 2. Selected oxidizing agents for direct radioiodination of peptides and proteins. PS = Polystyrene.

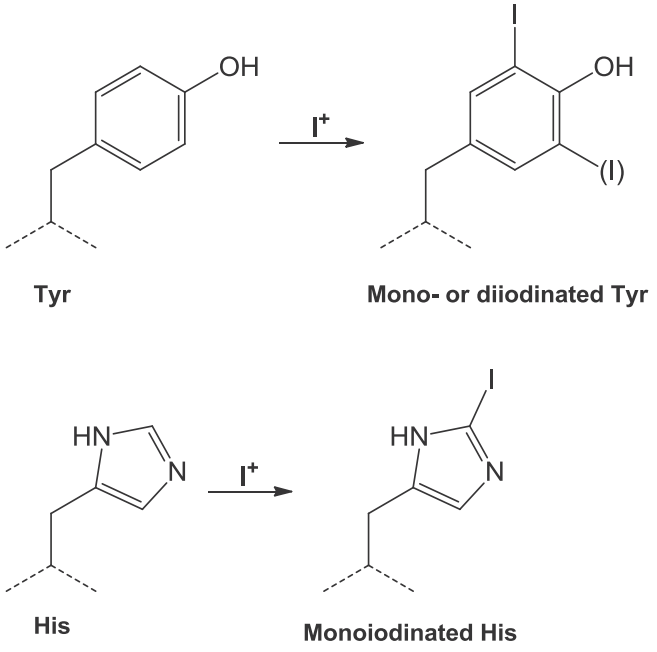

Fig. 3. Electrophilic substitution in tyrosine and in histidine by I^+.

Convenience and commercial availability of reagents (Pierce Iodination Beads) make Iodobeads a reliable alternative for radioiodination of peptides [36,37]. To avoid side reactions resulting from severe oxidizing conditions the use of milder solid-phase oxidizing agents such as Iodogen pre-coated tubes, where no reducing agent is needed and the reaction can be simply stopped by physical separation of Iodogen from the aqueous media, is highly attractive and has been preferred for the radioiodination of antibodies and their fragments.

Other oxidants frequently employed for radioiodination of sensitive substrates are organic peracids, whose main advantage is the fact that no chlorinated products or by-products resulting from over-oxidation are formed. Generally, peracids are formed *in situ* by reacting hydrogen peroxide with an organic acid (*e.g.* formic or acetic acid). In this case the concentration of the oxidizing agent can be kept very low, leading to mild labelling [38]. However, the radiochemical yields obtained with peracids are usually lower than those obtained using *N*-halooxidants [39].

Also, the use of an enzyme-catalyzed process to generate the active iodine species constitutes a mild alternative to the above referred chemical methods [40]. Peroxidase enzymes, in particular lactoperoxidase, which produces electrophilic radioiodine in the

presence of hydrogen peroxide, have also been used in the enzymatic direct radioiodination of peptides [41,42]. Self-radioiodination of lactoperoxidase may occur during the radioiodination procedure leading to lower labelling yields and making separation of labelled peptide from labelled enzyme more difficult. One way to overcome this problem is the use of lactoperoxidase covalently bound to an insoluble matrix, such as Sephadex beads. The Enzymobead iodination kit (Bio-Rad laboratories), an immobilized preparation of lactoperoxidase and glucose oxidase, has been successfully used in the radioiodination of several peptides and antibodies [42–46]. Although this method is technically demanding and more difficult to optimize, the probability of denaturation and/or oxidation of peptides or proteins is lower as compared to the chloramine-T or similar methods.

Indirect labelling via prosthetic groups has emerged as an alternative strategy in cases where direct labeling is not possible, namely in the case were the biological activity of the peptide may be disturbed by the harsh oxidizing conditions used in direct iodination or when molecular modifications, such as adding Tyr or replacing Phe with Tyr, are not feasible. For instance, oxidative reagents may cause oxidation of sensitive amino acids, like Trp to oxindole and Met to sulfoxide [47]. Despite the limited use of prosthetic groups, they are quite promising for radioiodination of peptide-based radiopharmaceuticals.

In this radioiodination approach, a pre-labelled prosthetic group such as the *Bolton-Hunter reagent* [48] (*N*-succinimidyl-3-(4-hydroxy-5-[*I]iodophenyl)-propionate, Fig. 4) is used. The activated aromatic moiety is radioiodinated and conjugated to the peptide in a second step. One major drawback of radiodination via phenolic compounds is the fast deiodination observed *in vivo*. Therefore, to overcome the low *in vivo* stability of the Bolton-Hunter reagent other non-phenolic aromatic labeling reagents like *N*-succinimidyl-4-[*I]iodobenzoate (PIB), *N*-succinimidyl-3-[*I] iodobenzoate (SIB) or *N*-succinimidyl-5-[*I]iodo-3-pyridine carboxylate (SIPC) (Fig. 4) with higher *in vivo* stability have also been proposed [49–51]. Other radioiodinated maleimide derivatives, such as *N*-(2-aminoethyl)maleimide (IBM) or 1-(3-[*I] iodophenyl)maleimide (IPM) have also been reported as prosthetic groups in the radioiodination of peptides. [52,53].

Recently, Billaud and colleagues introduced the first bimodal fluorinated and iodinated prosthetic group, tetrafluorophenyl 4-fluoro-3-iodobenzoate (TFIB), as a suitable acylating agent for the labelling of a wide variety of primary amine-containing compounds (Fig. 5). [^{125}I]/[^{18}F]TFIB was successfully used to tag tumor-targeting peptides such as PEG$_3$[*c*(RGDyK)]$_2$ and NDP-MSH, targeting $\alpha_v\beta_3$ integrin and MC1R receptors, respectively. [54].

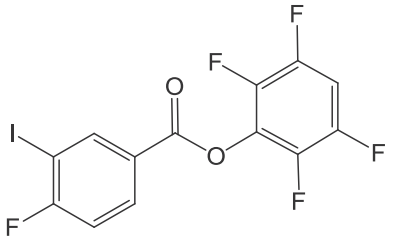

Fig. 5. Chemical structure of tetrafluorophenyl 4-fluoro-3-iodobenzoate (TFIB).

1.3. Determination of the chemical structure of radioiodinated compounds

In the past many radioiodinated compounds have been used without full structural characterization for radioimmunoassay (RIA) or imaging studies in nuclear medicine. However, some structural features of radioiodinated pharmaceuticals may alter the metabolic stability towards *in vivo* deiodination. The structure of the whole molecule, rather than just the radioiodination site, will affect the kinetics of deioiodination [55]. In recent years, some attempts have been made to correlate the metabolic dehalogenation rates of such pharmaceuticals with their structures and to determine, which structural features may hamper or favor metabolic deiodination [56].

The structure of the radioiodinated molecule and the site of radioiodine incorporation can usually be predicted with a reasonable degree of confidence in the different types of radioiodination reactions. However, when dealing with macromolecules with complex structures and multiple radioiodination sites it is more difficult to assign chemical structure of the labelled molecule.

The special features related to the radioactive compounds, such as the low molar concentration, associated to the low sensitivity presented by spectroscopic techniques do not allow their characterization by the conventional analytical methods currently used in chemistry. Therefore, the identification of the radioiodinated compounds is usually accomplished on the basis of similar studies (UV/vis, NMR, and IR spectroscopy, HPLC, and liquid chromatography/mass spectrometry) with the corresponding non-radioiodinated analogues previously obtained by means of suitable scale-up synthetic methods. Chromatographic techniques, mainly HPLC, can be readily used to characterize these radiolabelled molecules by comparison of their retention time (t_R) with those of the non-radioiodinated counterparts.

After the radioiodination procedure, it is of utmost importance

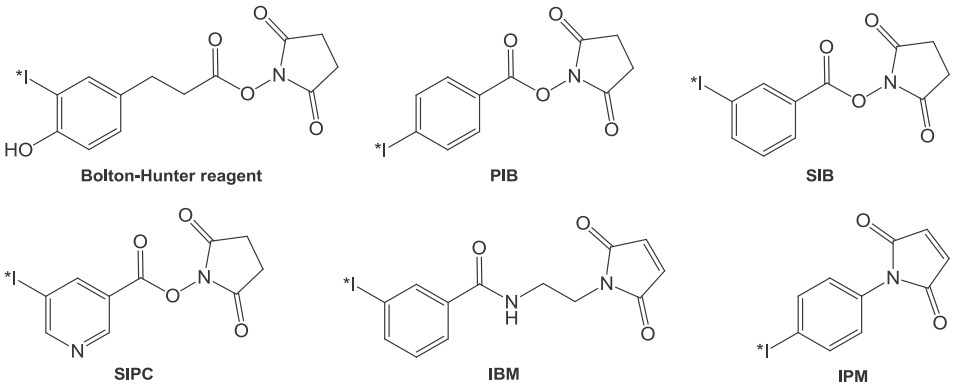

Fig. 4. Selected prosthetic groups for indirect radioiodination. PIB = *N*-succinimidyl-4-[*I]iodobenzoate, SIB = *N*-succinimidyl-3-[*I]iodobenzoate, SIPC = *N*-succinimidyl-5-[*I] iodo-3-pyridine carboxylate, IBM = *N*-(2-^{11}aminoethyl)maleimide and IPM = 1-(3-[*I]iodophenyl)maleimide. *I = $^{123or/125or/131}$I.

to remove excess precursor, unreacted radioiodide and by-products from the reaction mixture, using mainly chromatographic techniques. In the specific case of peptides, when their structure is known and there is only one labelling site, a simple elution by gel permeation chromatography (*e.g.* Sephadex G-50, G-25 or LH-20) with the appropriate solvent is generally sufficient to remove unreacted iodide [57–59]. Solid phase extraction with C18 cartridges has also been used to remove unreacted radioiodide [60]. However, a good separation of side products is not generally achieved because of some drawbacks associated to cartridge based technology. These include low separation efficiency due to small bed volume or a small capacity of the cartridge to separate the labelling mixture. On the other hand, UV and gama-detection monitoring is not possible and radiation exposure is higher due to direct handling. Compared to HPLC techniques, cartridges are only useful for single separations based on evident lipophilicity differences. HPLC is today the technique of choice for purification of radioiodinated peptides due to its easy performance and high separation efficiency [61].

2. Target-specific radioiodinated peptides

In this chapter we aim at highlighting the importance of radioiodinated peptides in biomedicine. The most exploited peptides for targeting relevant receptors *in vivo*, namely those related to cancer, will be reviewed and their main biomedical applications presented and discussed.

2.1. Targeting somatostatin (SST) receptor

Somatostatin (SST) is a cyclic peptide hormone that exists either as a 14 amino acid or a 28 amino acid variant (Fig. 1). Both amino acids 7–11 and the Cys-Cys disulphide bond, which confers a conformational constraint to the structure, are key for receptor binding. The very short biological life (3 min) of natural somatostatin, due to fast enzymatic degradation by endogeneous peptidases, prompted several research groups to modify the original peptide to enhance enzymatic stability while maintaining receptor binding affinity and biological activity. This optimization process resulted in the introduction of the cyclic synthetic octapeptide DPhe-Cys-Phe-DTrp-Lys-Thr-Cys-Thr-ol (octreotide or sandostatin, OC), in which D-amino acids were introduced and the ring size was decreased to the bioactive core sequence (Fig. 1). Octeotride preserved the 4-amino acid motif (Phe-DTrp-Lys-Thr) of native SST-14, which is the critical region for receptor binding, and presents enhanced stability towards enzymatic degradation. [62,63].

Somatostatin receptors are highly expressed in a variety of tumor cells and have been associated to neuroendocrine tumors, such as carcinoids, insulinomas and gastrinomas. To date, five subtypes of human somatostatin receptors ($SSTR_1$-$SSTR_5$) have been identified and cloned [64]. $SSTR_2$ is mainly found in primary tumors and metastases contrary to the other variants, which are strongly expressed in normal tissues as well.

^{123}I-labelled TOC (Fig. 1) ([^{123}I]TOC) was reported as the first imaging agent for sst-expressing primary tumors and metastases [26,27] and has been used to localize carcinoid tumors, pancreatic endocrine tumors, and paragangliomas [65]. However, clinical experience pointed to several drawbacks, namely stability issues and uptake in non-target tissues, providing evidence that a better imaging agent was still needed [66]. However, as [^{123}I]TOC was rapidly cleared via the hepatobiliary route, a substantial accumulation of radioactivity was observed in the intestines hampering the interpretation of planar and SPECT images of lesions in the abdominal region. Some of these problems could be solved by using a DTPA conjugated octreotide labelled with indium-111 ([^{111}In]OC). This radiopharmaceutical was approved in 1994 under the trade name Octreoscan® for clinical imaging of patients with neuroendocrine tumors.

Following earlier studies in which carbohydration was successfully applied to improve the biokinetics of $\alpha_v\beta_3$-integrin antagonists [67,68], radiolabelled glycated octreotides were introduced as a new series of SSTR-binding radiotracers with excellent physicochemical characteristics [69–71]. Thus, aiming to evaluate the effect of single C-terminal oxidation and simultaneous N-terminal carbohydration, the biological behaviour of [^{125}I]Tyr^3-octreotate ([^{125}I]TOCA) and maltotriose-[^{125}I]Tyr^3-octreotate ([^{125}I]Mtr-TOCA) was compared with that of [^{125}I]TOC in nude mice bearing AR42J tumor xenographs (Fig. 6) [71].

Contrary to [^{125}I]TOC, which displayed high biliary excretion, both radioiodinated octreotates were mainly cleared by the kidneys. Owing to the high tumor uptake and fast renal excretion excellent tumor to non-tumor ratios were observed with [^{125}I]Mtr-TOCA even for the well-known critical organs for [^{123}I]TOC scintigraphy, *i.e.* intestine, kidney and liver. The promising preclinical results prompted the same research group to perform human scintigraphic studies with [^{123}I]Mtr-TOCA in patients with ssr-positive tumors. [^{123}I]Mtr-TOCA scintigraphy enabled fast and high contrast imaging of SSTR-expressing tumors but showed no major advantage over Octreoscan® concerning maximum achievable tumor-to-tissue contrast and tumor detectability. Although patient absorbed doses were lower as compared to Octreoscan® scintigraphy, the limited activity retained within the tumor has hampered further therapeutic applications using the analogue [^{131}I]Mtr-TOCA [72].

Sugar conjugation of biooactive peptides has been shown to be a powerful tool to modulate peptide pharmacokinetics. The glucose ([^{125}I]Gluc-TOC), maltose ([^{125}I]Malt-TOC), and maltotriose ([^{125}I]Mtr-TOC) derivatives of [^{125}I]TOC (Fig. 6) were evaluated by Schotelius and colaborators in an effort to overcome the unfavourable kinetics of [^{125}I]TOC, *i.e* the low tumor retention and predominant hepatobiliar excretion [73].

Biodistribution studies in rat pancreatic (AR42J) xenografted mice showed that, when compared to the parent compound, [^{125}I]TOC, the carbohydrated tracers were rapidly excreted via the kidneys without increased renal uptake. Among all tested radiopeptides, [^{125}I]Gluc-TOC emerged as the one with the highest tumor accumulation in this animal model.

Later, in a comparative study using [^{125}I]Mtr-TOCA (net charge $z = +1$) and the neutral charge glycosylated [^{125}I]TOC analogues ($z = 0$) [^{125}I]Gluc-TOCA, [^{125}I]Gluc-S-TOCA and [^{125}I]Gal-S-TOCA (Fig. 6), Schotelius research group demonstrated that reduction of peptide net charge lead to reduced kidney accumulation without compromising receptor binding affinity. Moreover, glycosylation with small carbohydrates, especially in the case of Gluc-S moiety, has shown to be a very promising tool to improve pharmacokinetics of radiolabelled octreotides owing to the cumulative effects on tumor uptake and kidney excretion [74].

As mentioned before, radioiodinated peptides are usually susceptible to *in vivo* deiodination by endogeneous deiodinases because direct radioiodination occurs on a Tyr residue. To overcome this issue, Zalutsky and collaborators have developed octreotide and octreotate analogues with the radiohalogen located in a prosthetic group appended to the peptide N-terminal [75,76]. The radioiodinated peptides (Fig. 7), prepared in reasonable radiochemical yields by conjugation to radiohalogenated acylation agents, were resistant to dehalogenation and, most importantly, no alteration in receptor binding affinity was observed.

The second generation peptide N-(4-guanidinomethyl-3-iodobenzoyl)-Phe^1-octreotate (GMIBO) displayed a much higher intracellular accumulation *in vitro* than the analogue [^{125}I]Gluc-

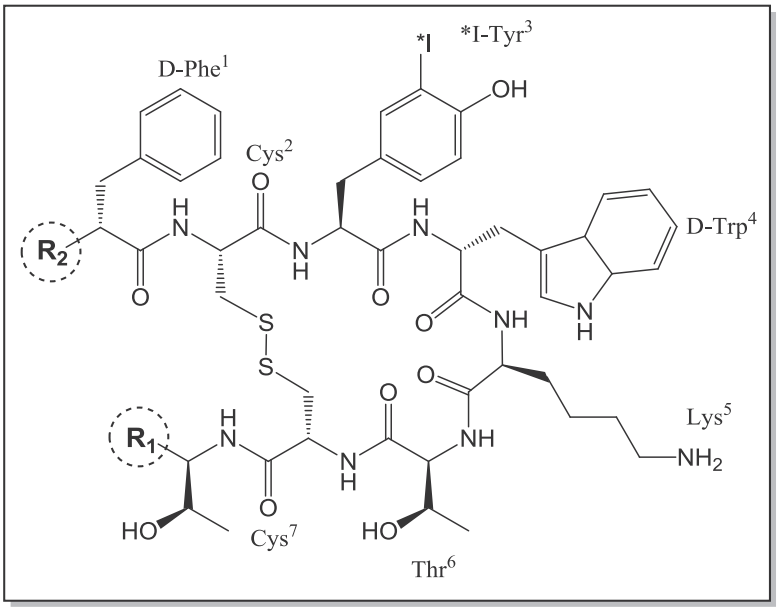

[*I]-TOC ($R_1 = CH_2OH$)
[*I]-TOCA ($R_1 = CO_2H$)
$R_2 = NH_2$

[*I]-Gluc-TOC ($R_1 = CH_2OH$)
[*I]-Gluc-TOCA ($R_1 = CO_2H$)
$R_2 =$

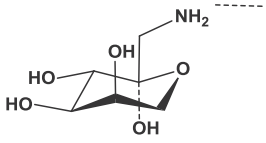

[*I]-Malt-TOC ($R_1 = CH_2OH$)
[*I]-Malt-TOCA ($R_1 = CO_2H$)
$R_2 =$

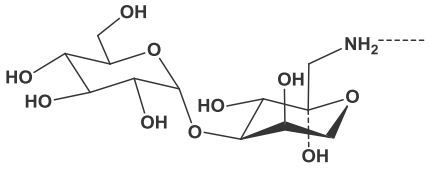

[*I]-Mtr-TOC ($R_1 = CH_2OH$)
[*I]-Mtr-TOCA ($R_1 = CO_2H$)
$R_2 =$

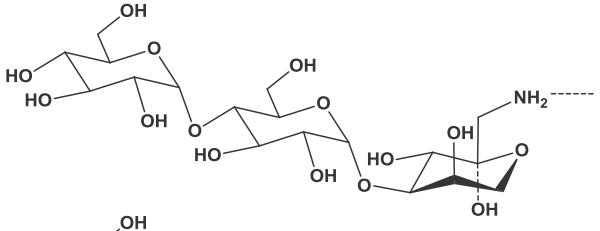

[*I]-Gluc-S-TOCA ($R_1 = CO_2H$) $R_2 =$

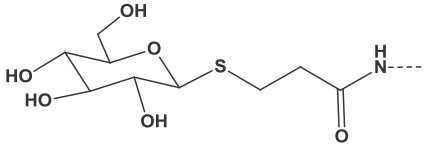

[*I]-Gal-S-TOCA ($R_1 = CO_2H$) $R_2 =$

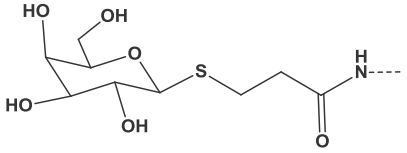

Fig. 6. Chemical structure of the carbohydrate derivatives of [^{125}I]TOC and [^{125}I]TOCA. *I = $^{123/125}$I.

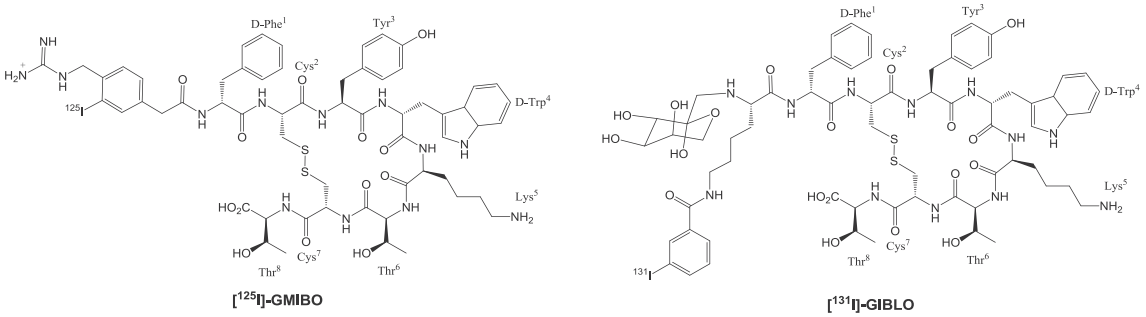

Fig. 7. Chemical structures of radioiodinated octreotates [^{125}I]GMIBO and [^{131}I]GIBLO.

TOCA (Fig. 6) [76]. However, the higher accumulation of [^{125}I]GMIBO in normal tissues, particularly in the liver and kidney has precluded the clinical application of its ^{131}I-labelled version for systemic radiotherapy.

The octreotate analogue containing both a sugar moiety and a non-tyrosine prosthetic group for radioiodination N^{α}-(1-deoxy-D-fructosyl)-N^{ε}-(3-iodobenzoyl)-Lys^0-octreotate (GIBLO) (Fig. 7) maintained high affinity to sstr2 and exhibited a lower deiodination rate than I-Gluc-TOCA [77]. Internalization features of the radioiodinated analogue [^{131}I]GIBLO *in vitro* and tumor uptake *in vivo*, while inferior to that of [^{131}I]Gluc-TOCA, were similar to those of [^{131}I]TOC suggesting the need of alternative strategies for enhancing cellular trapping of radioiodine and further improving pharmacokinetics.

There is recent *in vitro* and *in vivo* evidence that $SSTR_2$ antagonists are better tools to target neuroendocrine tumors (NET) than $SSTR_2$ agonists [78], which makes radiolabeled $sstr_2$-antagonists particularly attractive for targeting those tumors. Indeed, antagonists bind to a greater number of $sstr_2$ sites than agonists. In a recent study from Reubi and colleagues, the second-generation $SSTR_2$-antagonist JR11(DOTA-Cpa-*c*[DCys-Aph(Hor)-DAph(Cbm)-Lys-Thr-Cys]-DTyr-NH_2; Cpa = *p*-chlorophenylalanine; Aph(Hor) = 4-amino-L-hydroorotyl-phenylalanine; Aph(Cbm) = 4-amino-carbamoyl-phenylalanine) was labelled with ^{125}I and compared with [^{125}I]TOC in a wide range of non-NET and NET [79]. *In vitro* data has revealed a markedly higher binding of [^{125}I]JR11 versus [^{125}I]TOC in some tumors known to express little or no $sstr_2$, namely renal cell cancers, breast carcinomas, medullary thyroid cancer, and non-Hodgkin lymphoma. These findings suggested that $SSTR_2$ targeting with this kind of antagonists should also be seriously considered in other types of malignancies beyond NET.

2.2. Targeting the vasoactive intestinal peptide receptor (VPAC-1)

Vasoactive intestinal peptide (VIP, His-Ser-Asp-Ala-Val-Phe-Thr-Asp-Asn-Tyr [10]-Thr-Arg-Leu-Arg-Lys-Gln-Met-Ala-Val-Lys-Lys-Tyr [22]-Leu-Asn-Ser-Ile-Leu-Asn-NH_2) is a 28 amino acid neuropeptide, isolated in the early 1970s from the small intestine of the hog. It belongs to the glucagon-secretin family and displays a wide range of biological activities [80]. In addition to its relevant vasodilatory properties, VIP also stimulates the secretion of several hormones and promotes the growth and proliferation of normal and tumor cells [81,82].

The actions of VIP are mediated by two cell surface subtype receptors, VPAC1 and VPAC2, which, particularly in the case of the VPAC1, are expressed in the great majority of the most frequently occurring human tumors, including breast (100%), prostate (100%), urinary bladder (100%), colon (96%), pancreatic (65%), lung (58%), stomach (54%) and liver (49%) cancer as well as meningiomas (100%) and lymphomas (58%). [82].

The higher expression of VIP receptors in various tumor cells as compared with normal peripheral blood cells or tissues [83] has provided the basis for the clinical use of radiolabeled VIP for *in vivo* localization of intestinal adenocarcinomas and endocrine tumors [84].

The two tyrosine residues at positions 10 and 22 in VIP scaffold are suitable for direct labelling with radioiodine. Consequently, VIP has been successfully radioiodinated with ^{123}I according to a modification of the iodogen method and [^{123}I]VIP scintigraphy was used to image gastrointestinal tumors. The first clinical trial with [^{123}I]VIP that enrolled 79 patients with gastrointestinal tumors expressing VIP receptors was reported by Virgolini et al. in 1994. In this study, primary tumors and metastases were detected shortly after administration of the radiopeptide and were still visible 24 h post injection [84].

In a series of subsequent clinical trials, [^{123}I]VIP was used to image different types of tumors, including colorectal [85], pancreatic [86], VIPomas [87], and endocrine tumors [88]. In these imaging studies VIP scintigraphy showed an advantage over CT conventional scanning in patients with small carcinoid tumors due especially to the [^{123}I]VIP scan sensitivity found for primary or recurrent carcinomas.

In spite of the promising potential of [^{123}I]VIP to localize small tumors and its usefulness for early diagnosis of cancer, naturally occurring VIP analogues display several limitations concerning *in vivo* imaging due to its short biological half-life and fast degradation in liver and kidneys that greatly limits its clinical application. Chemical modification of native peptide is still needed to overcome this metabolic instability.

2.3. Targeting the $\alpha_v\beta_3$ integrin receptor

Integrins are transmembrane heterodimeric glycoprotein receptors consisting of an α- and a β-subunit that regulate many important biological processes such as cell adhesion, migration and invasion, cell growth and differentiation, and apoptosis. The role of integrins in the regulation of angiogenesis is an essential feature in tumor progression and metastatic dissemination. The α_v integrins form a subfamily of five members ($\alpha_v\beta_1$, $\alpha_v\beta_3$, $\alpha_v\beta_5$, $\alpha_v\beta_6$ and $\alpha_v\beta_8$) that recognizes a group of overlapping ligands, which generally contain the canonical tripeptide recognition sequence Arg-Gly-Asp (RGD) [89,90]. Among them, $\alpha_v\beta_3$ integrin has been the most extensively studied, and many probes targeting it have been developed [91]. The $\alpha_v\beta_3$ integrin, comprising a 125-kDa α_v subunit and a 105-kDa β_3 subunit, binds to a wide variety of extracellular matrix proteins, such as vitronectin, fibrinogen, laminin or collagen [92,93].

The discovery of the RGD pharmacophore, which still represents the scaffold most commonly employed for $\alpha_v\beta_3$ targeting, encouraged research on small peptide-based $\alpha_v\beta_3$ antagonists for

antiangiogenic therapy [94]. Moreover, a wide spectrum of RGD-containing peptides has been labelled with a variety of radionuclides aiming at the non-invasive visualization and quantification of $\alpha_v\beta_3$-integrin expression levels before, during, and after anti-angiogenic therapy [95–101]. The most relevant radioiodinated RGD peptides targeting $\alpha_v\beta_3$ integrins are summarized in Table 2.

In the search for small RGD integrin antagonists Kessler and colleagues have identified *cyclo*(-Arg-Gly-Asp-DPhe^4-Val^5-) (*c*(RGDfV)) as a selective $\alpha_v\beta_3$ antagonist with binding affinities within the low nanomolar range [94,102]. Structure-activity relationship (SAR) studies have also shown that, besides the essential RGD sequence, a hydrophobic amino acid in position 4, such as Phe, could increase the affinity of the peptide towards $\alpha_v\beta_3$ [105]. By contrast, the amino acid in position 5 did not show any influence on the biological activity.

Haubner et al. designed a family of cyclic RGD peptides where the possible sites for modification were the amino acids in positions 4 and 5. Hence, *D*-Phe^4 or Val^5 were replaced by a Tyr residue, resulting in *cyclo*(-Arg-Gly-Asp-DTyr^4-Val^5-) (*c*(RGDyV)) or *cyclo*(-Arg-Gly-Asp-DPhe^4-Tyr^5-) (*c*(RGDfY)), respectively (Fig. 8) [103]. Introduction of tyrosine in the peptide sequence has allowed electrophilic radioiodination using the iodogen method (*e.g.* ^{125}I) giving [^{125}I]-*c*(RGDyV) and [^{125}I]-*c*(RGDfY), respectively.

The radioiodinated peptides were evaluated biologically in biodistribution studies in melanoma M21-bearing nude mice and osteosarcoma-bearing BALB/c mice. [^{125}I]-*c*(RGDyV) exhibited the highest affinity and selectivity for $\alpha_v\beta_3$ integrins *in vitro* and receptor-specific tumor accumulation *in* vivo (Fig. 8). However, a predominant hepatobiliary excretion together with a relatively high liver and intestines uptake precluded clinical application for tumor imaging.

Aiming to improve pharmacokinetics and clearance through the kidneys a modified derivative of *c*(RGDyV) the pentapeptide *cyclo*(-Arg-Gly-Ala-Asp-DTyr^4-Lys^5-) *c*(RGDyK), in which Val^5 was replaced by Lys^5, was glycosylated by conjugation of a glucose-based sugar amino acid (SAA) to the ε-amino function of the lysine residue (Fig. 8) [67]. The introduction of this sugar moiety has improved the pharmacokinetic behaviour of [^{125}I]-*c*(RGDfY) by decreasing lipophilicity and hepatic uptake. Also, this second-generation tracer [^{125}I]-*c*(RGDyK(SAA)) showed high tumor uptake and good tumor-to-non-target organ ratios that allowed non-invasive visualization of $\alpha_v\beta_3$-expressing tumors. The replacement of Val in *c*(RGDyV) by a lysine residue has allowed the preparation of [^{125}I]-*c*(RGDyK), which increased the tracer hydrophilicity as reflected in a faster blood clearance and decreased uptake and retention in the liver when compared to [^{125}I]-*c*(RGDyV). The tracer revealed rapid tumor uptake in a subcutaneous gliobastoma U87MG model but the prolonged kidney retention limited further clinical application [104].

It is well established that covalent binding of polyethylene glycol (PEG) to therapeutic peptides leads in general to improvement of pharmacokinetic, immunogenic and antigenic profiles of those peptides. PEGylation of *c*(RGDyK) was accomplished by reaction of the active succinimidyl ester (NHS) of mono-methoxypoly(ethylene glycol)(mPEG)-propionate with the ε-amino group of the lysine residue under basic conditions, yielding the pegylated derivative *c*(RGDyK)-mPEG [104]. The pharmacokinetics and targeting potential of the latter were compared with the corresponding precursor [^{125}I]-*c*(RGDyK) in a U87MG gliobastoma xenografted mouse model, and it has been concluded that PEGylation led to a drastically decreased renal uptake, slightly increased liver accumulation and prolonged tumor retention.

Most recently, a new strategy for the radioiodination of RGD-peptides was introduced by Ogawa et al. [106] The RGD-containing peptide *c*-(RGDfK) was used in their study as a model for establishing a novel ^{211}At-labelling method for peptides. The radioiodinated peptide [^{125}I]-*c*(RGDfK) was prepared from a precursor containing a tributylstannyl group on the phenylalanine residue.

SAR studies have demonstrated that incorporation of N$^{\alpha}$-methylated amino acids into different biologically relevant peptides led to peptidomimetics with enhanced biological properties [107–109] as found for Cilengitide (EMD121974, Fig. 8), a promising integrin αvβ3 antagonist that failed Phase III clinical trial on treating glioblastoma [104].

Aiming to obtain clinically relevant targeted SPECT imaging agents for angiogenesis Bianchini and colleagues developed a cilengitide-like RGD-cyclopentapeptide containing the cyclic amino acid (R)morpholine-3-carboxylic acid (Fig. 8) [110,111]. Replacement of DPhe with DTyr allowed for labelling this cilengitide-like RGD-cyclopentapeptide with ^{125}I by the method of chloramine-T. The resulting radioiodinated RGD-cyclopentapeptide, [^{125}I]-[*c*RGDy-(3S)-Carboxymorpholine], has shown to interact *in vivo* with $\alpha_v\beta_3$ integrin expressed by melanoma cells. Images obtained from a hybrid small-animal micro-SPECT/CT imaging system clearly showed the ability of the ^{125}I-labelled cilengitide-like RGD to monitor the growth of melanoma xenografts (Fig. 9). Co-injection of the tracer with the corresponding unlabeled ligand showed high selectivity for $\alpha_v\beta_3$ expressing tumor cells. Moreover, the observed high retention of radioactivity within the tumor together with a high tumor/background ratio, and the selectivity for $\alpha_v\beta_3$ expressing tumor cells suggested that ^{125}I-labelled morpholine-based RGD-cyclopentapeptides might play a key role in future therapeutic strategies for management of $\alpha_v\beta_3$ positive tumors.

Table 2
RGD peptides and radioiodinated derivatives targeting $\alpha_v\beta_3$ integrins.

	Peptide amino acid sequence	reference
c(RGDfV)	cyclo(-Arg-Gly-Asp-DPhe^4-Val^5-)	[94,102]
c(RGDyV)	cyclo(-Arg-Gly-Asp-DTyr^4-Val^5-)	[103]
[^{125}I]-*c*(RGDyV)	[^{125}I]-3-iodo-DTyr [4]-cyclo(-Arg-Gly-Asp-DTyr^4-Val^5-)	[103]
c(RGDfY)	cyclo(-Arg-Gly-Asp-DPhe^4-Tyr^5-)	[103]
[^{125}I]-*c*(RGDfY)	[^{125}I]-3-iodo-DTyr [5]-cyclo(-Arg-Gly-Asp-DPhe^4-Tyr^5-)	[103]
c(RaDYV)	cyclo(-Arg-DAla-Asp-Tyr^4-Val^5-)[a]	[103]
[^{125}I]-*c*(RaDYV)	[^{125}I]-3-iodo-Tyr [4]-cyclo(-Arg-DAla-Asp-Tyr^4-Val^5-)[a]	[103]
c(RGDyK(SAA))	cyclo(-Arg-Gly-Asp-DTyr^4-Lys^5(SAA)-)	[67]
[^{125}I]-*c*(RGDyK(SAA))	[^{125}I]-3-iodo-Tyr [4]-cyclo(-Arg-Gly-Asp-DTyr^4-Lys^5(SAA)-)	[67]
c(RGDyK)	cyclo(-Arg-Gly-Asp-DTyr^4-Lys^5-)	[104]
[^{125}I]-*c*(RGDyK)	[^{125}I]-3-iodo-Tyr [4]-cyclo(-Arg-Gly-Asp-DTyr^4-Lys^5-)	[104]
[^{125}I]-*c*(RGDyK)-mPEG	[^{125}I]-3-iodo-Tyr [4]-cyclo(-Arg-Gly-Asp-Tyr^4-Lys^5-)-mPEG	[104]

Lower case letters designate D*-amino acids.*
[a] [^{125}I]-*c*(RaDYV) was used as a negative control for nonspecific binding quantification.s.

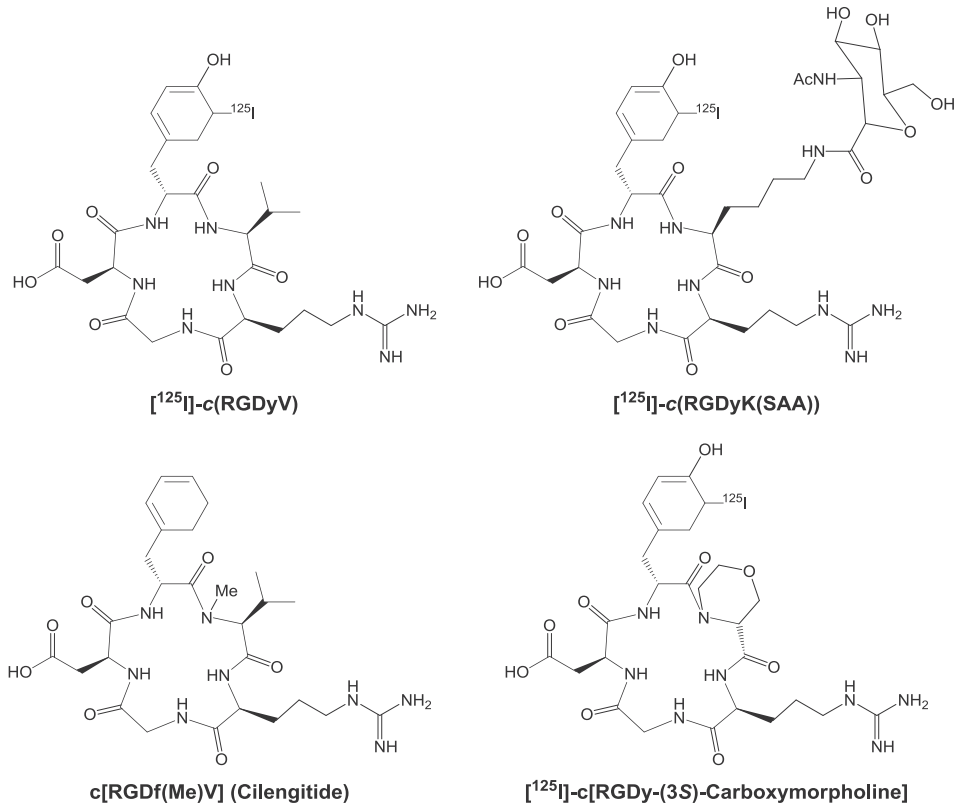

Fig. 8. Schematic structures of the first generation tracer [^{125}I]-*c*(RGDfV) and its glycosylated analogue [^{125}I]-*c*(RGDyK(SAA)) [67,103], Cilengitide and ^{125}I-labelled cilengitide-like RGD-cyclopentapeptide, [^{125}I]-*c*[RGDy-(3S)-Carboxymorpholine].

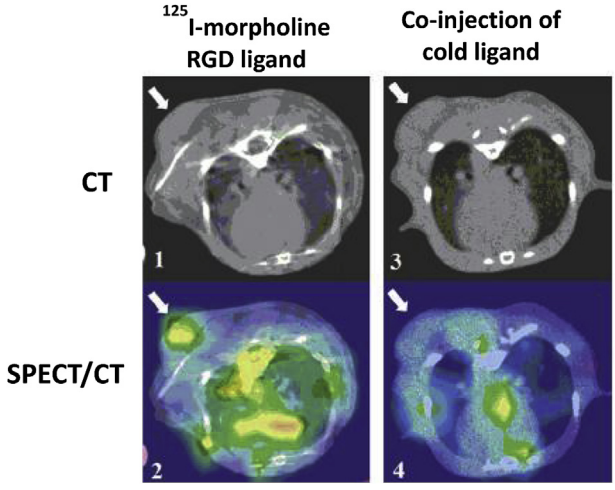

Fig. 9. Transaxial slices through mouse chest at implanted melanoma tumor level (arrows). In upper panels CT images, in lower panels fused SPECT/CT images. Images were acquired at 40 min after tail vein injection of the radioiodinated morpholine RGD ligand (250 μCi in 0.2 mL of saline). The displacement study was achieved with an excess of cold ligand (18 mg/kg) injected 10 min before the tracer. Adapted with permission from Bianchini et al. Copyright 2012. American Chemical Society [111].

Click chemistry has been successfully applied in the development of combinatorial libraries containing the triazole ring, which mimics the amide bond in peptidomimetics chemistry. This synthetic strategy was used for generating RGD mimetics of cilengitide by combining azides and alkynes bearing Asp and Arg isosteres, respectively. Thus, the triazole ring was devised as a mimetic of glycine acting as a spacer. Alkynes with different chain lengths and molecular shapes were introduced as isosteres of arginine, whereas azides bearing a carboxylic group and an aromatic ring were considered as mimetics of Asp and DPhe moieties, respectively. Using this approach, Trabocchi et al. designed and evaluated a family of triazole-containing RGD peptidomimetics synthesized by means of a Cu(I)-catalyzed 1,3-dipolar alkyne-azide coupling reaction (Fig. 10), some of which displayed relevant binding affinities towards $\alpha_v\beta_3/\alpha_v\beta_5$ integrins in solid-phase receptor assays [112].

Among all of the triazole peptidomimetics of the RGD sequence a guanidine based triazole-containing RGD peptidomimetic (GuRGD, Fig. 10) displayed the highest binding affinity toward $\alpha_v\beta_3$ and $\alpha_v\beta_5$ and has been selected for subsequent molecular modelling studies. A docking simulation using the available crystallographic data of $\alpha_v\beta_3$ integrin revealed a RGD-like binding mode toward $\alpha_v\beta_3$ integrin also showing a key interaction between the triazole ring and Tyr^{178} side chain in the binding region of $\alpha_v\beta_3$.

Biological studies have also demonstrated that this RGD peptidomimetic was able to inhibit the adhesion of integrin-rich human melanoma cells to RGD-proteins, such as vitronectin, fibronectin, and osteopontin. Inhibition of angiogenesis was also confirmed in *in vitro* and *in vivo* experimental models. Overall, these findings seem to indicate the potential role of GuRGD as an antiangiogenic agent in the diagnosis and therapy of $\alpha_v\beta_3$ integrin expressing tumors.

Following these promising results the same researchers devised the application of this RGD mimetic as a novel SPECT/PET imaging agent by exploring diverse positions for labelling with iodine radionuclides [113]. Thus, GuRGD was structurally modified by replacing the phenyl ring with a phenol group (*e.g.* [^{125}I]GuRGD, [^{125}I]PyrRGD, [^{125}I]BZMRGD) or by alkylating the guanidine moiety with a tyramine pendant group, such as in [^{125}I]TyrRGD, in order to introduce an iodine atom on the aromatic ring (Fig. 10). Moreover,

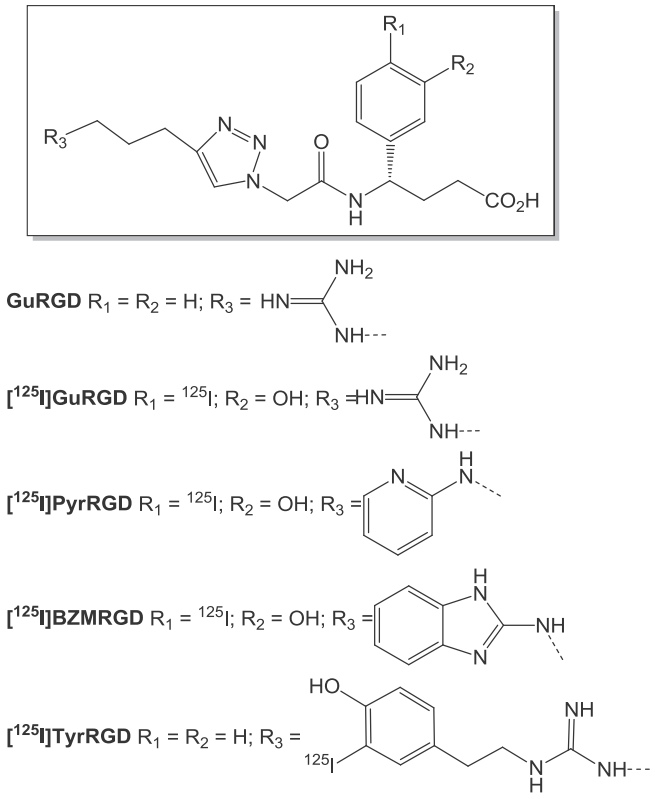

Fig. 10. Struture of a guanidine based triazole-containing RGD peptidomimetic (GuRGD) and of radioiodinated RGD mimetic ligands containing guanidine ([^{125}I]GuRGD), pyridine ([^{125}I]PyrRGD) and benzimidazole ([^{125}I]BZMRGD) moieties and the tyramine linkage ([^{125}I]TyrRGD).

the modulation of the guanidine bioisostere, by insertion of benzimidazole and aminopyridine moieties as arginine bioisosteres was undertaken to explore the structure–activity relationship of the compounds *in vivo* and to better understand the biological role of the guanidine moiety in the pharmacokinetic and pharmacodynamic profiles of the radioligands.

The ability of the iodinated RGD peptidomimetics for binding $\alpha_v\beta_3$ integrin was tested in a solid-phase competitive binding assay. IC_{50} values revealed that all the iodinated compounds displayed higher binding affinity towards $\alpha_v\beta_3$ integrin as compared to their corresponding non-labelled precursors. It is noteworthy that the guanidine substitution in the arginine mimetic portion, with either 2-aminopyridine ([^{125}I]PyrRGD) or 2-aminobenzimidazole ([^{125}I]BZMRGD) moieties, resulted in higher binding affinities. Based on binding affinity and molecular modelling studies, [^{125}I]GuRGD, [^{125}I]PyrRGD and [^{125}I]BZMRGD were evaluated in mice bearing melanoma xenografts of human origin. SPECT images evidenced clearly the ability of the ^{125}I–labelled RGD peptidomimetics to visualize the melanoma xenotransplants (Fig. 11).

2.4. Targeting the glucagon-like peptide 1 (GLP-1)

Glucagon-like peptide 1 (GLP-1) is a peptide hormone responsible for insulin release from the β-cells in the pancreas. The insulinotropic action of GLP-1 is mediated by a specific receptor that is mainly expressed in the islets of Langerhans. The glucagon-like peptide-1 receptor (GLP-1R), which is a member of the G-protein-coupled receptor family (GPCR), is an important target due to its high expression density on the surface of more than 90% of benign insulinomas, some malignant insulinomas, most gastrinomas, and most phaeochromocytomas [114].

Although the peptide GLP-1(1–37) has been initially identified as the post-translational cleavage product of the proglucagon gene [115], the two N-terminally truncated products GLP-1(7–37) and GLP-1(7–36)NH_2 were identified as the active species that recognized the pancreatic receptor (Table 3) [116] and references therein.

Several radioligands targeting the GLP-1R have been successfully employed for imaging benign insulinomas and have shown promising results in preclinical studies. The development of these targeting probes has relied mostly on two distinct approaches, either using the human GLP-1(7–36) NH_2 peptide as the ligand or using the agonist exendin isolated from the venom of the lizard Gila monster. Some of the most relevant GLP-1 analogues are presented in Table 3.

Early preclinical data has demonstrated the ability of ^{125}I-labelled GLP-1(7–36)NH_2, presumably radioiodinated on the Tyr^{19} residue, to image insulinoma *in vivo* in a rat model [117]. However, the clinical application of this tracer has been hampered by its low stability.

GLP-1 is degraded rapidly by dipeptidyl peptidase IV (DDP IV), which cleaves the GLP-1 N-terminal sequence (HAE). The search for analogues with higher stability led to the identification of the GLP-1R agonists exendin-3 (Exe-3) and exendin-4 (Exe-4) [118,119]. These two 39-amino acid natural peptides, which are metabolically resistant, share nearly 50% homology with the human GLP-1. Exendin-4 only differs from exendin-3 by two amino acid substitutions, Gly^2-Glu^3 in place of Ser^2-Asp^3. However, these subtle structural differences determine their distinct pharmacological properties.

The use of ^{125}I-labelled exendin-3 for detection of insulinomas

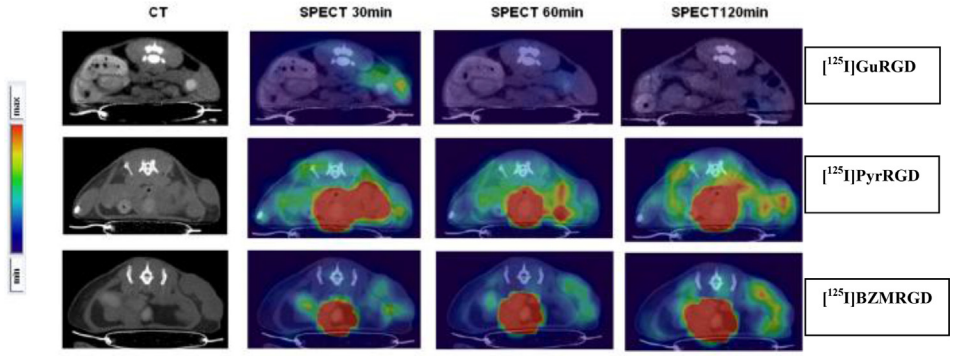

Fig. 11. Biodistribution studies of [^{125}I]GuRGD, [^{125}I]PyrRGD and [^{125}I]BZMRGD in human melanoma xenografts. Upper panel: SPECT/CT transaxial slices taken at the tumor level at different time points, representative images of one mouse (n = 3). Adapted with permission from Bianchini et al. Copyrigth 2015 Elsevier Ltd [113].

Table 3
GLP-1 analogues and their radioiodinated analogues.

Amino acid sequence:
GLP-1(1-37)
His-^{1}Asp-Glu-Phe-Glu-Arg-His^{7}-Ala-Glu-Gly-Thr-Phe-Thr-Ser-Asp-Val-Ser-Ser-Tyr^{19}-Leu-Glu-Gly-Gln-Ala-Ala-Lys-Glu-Phe-Ile-Ala-Trp-Leu-Val-Lys-Gly-Arg^{36}-Gly
GLP-1(7-37)
His^{7}-Ala-Glu-Gly-Thr-Phe-Thr-Ser-Asp-Val-Ser-Ser-Tyr^{19}-Leu-Glu-Gly-Gln-Ala-Ala-Lys**^{26}**-Glu-Phe-Ile-Ala- Trp-Leu-Val-Lys^{34}-Gly-Arg^{36}-Gly
Liraglutide
H-His^{7}-Ala-Glu-Gly-Thr-Phe-Thr-Ser-Asp-Val-Ser-Ser-Tyr^{19}-Leu-Glu-Gly-Gln-Ala-Ala-Lys^{26}(γ-Glu-palmitoyl)-Glu-Phe-Ile-Ala-Trp-Leu-Val-Arg^{34}-Gly-Arg-Gly-OH
[^{125}I]Liraglutide
H-His^{7}-Ala-Glu-Gly-Thr-Phe-Thr-Ser-Asp-Val-Ser-Ser-[^{125}I]Tyr^{19}-Leu-Glu-Gly-Gln-Ala-Ala-Lys^{26}(γ-Glu-palmitoyl)-Glu-Phe-Ile-Ala-Trp-Leu-Val-Arg^{34}-Gly-Arg-Gly-OH
GLP-1(7-36)NH$_2$
His^{7}-Ala-Glu-Gly-Thr-Phe-Thr-Ser-Asp-Val-Ser-Ser-Tyr^{19}-Leu-Glu-Gly-Gln-Ala-Ala-Lys-Glu-Phe-Ile-Ala-Trp-Leu-Val-Lys-Gly-Arg^{36}-NH$_2$
[^{125}I]**GLP-1(7-36)NH$_2$**
His^{7}-Ala-Glu-Gly-Thr-Phe-Thr-Ser-Asp-Val-Ser-Ser-[^{125}I]Tyr^{19}-Leu-Glu-Gly-Gln-Ala-Ala-Lys-Glu-Phe-Ile-Ala-Trp-Leu-Val-Lys-Gly-Arg^{36}-NH$_2$
Exendin-3
His^{1}-Ser^{2}-Asp^{3}-Gly-Thr-Phe-Thr^{7}-Ser-Asp-Leu-Ser-Lys-Gln-Met-Glu-Glu-Glu-Ala-Val-Arg-Leu-Phe-Ile-Glu-Trp-Leu-Lys^{27}-Asn-Gly-Gly-Pro-Ser-Ser-Gly-Ala-Pro-Pro-Pro-Ser^{39}-NH$_2$
[^{125}I]**Exendin-3**
[^{125}I]His^{1}-Ser^{2}-Asp^{3}-Gly-Thr-Phe-Thr^{7}-Ser-Asp-Leu-Ser-Lys-Gln-Met-Glu-Glu-Glu-Ala-Val-Arg-Leu-Phe-Ile-Glu-Trp-Leu-Lys^{27}-Asn-Gly-Gly-Pro-Ser-Ser-Gly-Ala-Pro-Pro-Pro-Ser^{39}-NH$_2$
Exendin-4 (Exenatide)
His^{1}-Gly^{2}-Glu^{3}-Gly-Thr-Phe-Thr-Ser-Asp-Leu-Ser-Lys-Gln-Met-Glu-Glu-Glu-Ala-Val-Arg-Leu-Phe-Ile-Glu-Trp-Leu-Lys^{27}-Asn-Gly-Gly-Pro-Ser-Ser-Gly-Ala-Pro-Pro-Pro-Ser^{39}-NH$_2$
[^{125}I]Exendin-4
[^{125}I]His^{1}-Gly^{2}-Glu^{3}-Gly-Thr-Phe-Thr-Ser-Asp-Leu-Ser-Lys-Gln-Met-Glu-Glu-Glu-Ala-Val-Arg-Leu-Phe-Ile-Glu-Trp-Leu-Lys^{27}-Asn-Gly-Gly-Pro-Ser-Ser-Gly-Ala-Pro-Pro-Pro-Ser^{39}-NH$_2$
[^{125}I]-[Tyr^{39}]exendin-4
H-His-Gly-Glu-Gly-Thr-Phe-Thr-Ser-Asp-Leu-Ser-Lys-Gln-Met-Glu-Glu-Glu-Ala-Val-Arg-Leu^{21}-Phe^{22}-Ile^{23}-Glu-Trp-Leu-Lys-Asn-Gly-Gly-Pro-Ser-Ser-Gly-Ala-Pro-Pro-Pro-[^{125}I]Tyr^{39}-NH$_2$
[Nle^{14},[^{125}I]-Tyr^{40}-NH$_2$]Ex-4
His^{1}-Gly^{2}-Glu^{3}-Gly-Thr-Phe-Thr-Ser-Asp-Leu-Ser-Lys-Gln-Nle^{14}-Glu-Glu-Glu-Ala-Val-Arg-Leu-Phe-Ile-Glu-Trp-Leu-Lys^{27}-Asn-Gly-Gly-Pro-Ser-Ser-Gly-Ala-Pro-Pro-Pro-Ser^{39}-[^{125}I]Tyr^{40}-NH$_2$
Exendin(9-39)NH$_2$ antagonist
H-Asp^{9}-Leu-Ser-Lys-Gln-Met-Glu-Glu-Glu-Ala-Val-Arg-Leu-Phe-Ile-Glu-Trp-Leu-Lys^{27}-Asn-Gly-Gly-Pro-Ser-Ser-Gly-Ala-Pro-Pro-Pro-Ser^{39}-NH$_2$
[^{125}I]BH-exendin(9–39) antagonist [[^{125}I]BH-Lys^{27}]Ex(9-39)NH$_2$
H-Asp^{9}-Leu-Ser-Lys-Gln-Met-Glu-Glu-Glu-Ala-Val-Arg-Leu-Phe-Ile-Glu-Trp-Leu-[^{125}I-BH]-Lys^{27}-Asn-Gly-Gly-Pro-Ser-Ser-Gly-Ala-Pro-Pro-Pro-Ser^{39}-NH$_2$
[Nle^{14},[^{125}I]-Tyr^{40}-NH$_2$]Ex(9-39) antagonist
H-Asp^{9}-Leu-Ser-Lys-Gln-Nle^{14}-Glu-Glu-Glu-Ala-Val-Arg-Leu-Phe-Ile-Glu-Trp-Leu-Lys^{27}-Asn-Gly-Gly-Pro-Ser-Ser-Gly-Ala-Pro-Pro-Pro-Ser^{39}-[^{125}I]Tyr-^{40}NH$_2$

was firstly reported by Gotthardt et al. Owing to the lack of Tyr in its structure, exendin-3 was radioiodinated with ^{125}I on His^{1}. However, when compared to ^{125}I-labelled GLP-1, radioiodinated exendin-3 showed a more pronounced maximal pancreatic and tumor uptake in a rat insulinoma model and offered better visualization of tumors, possibly due to its higher stability. [117].

Several exendin-4 based probes have been reported to be suitable candidates for SPECT or PET imaging studies [120–128]. However, exendin-4 based PET tracers suffered from high kidney uptake and low specific activity that resulted in high radiation doses to the kidney, poor image contrast, and potential safety issues due to hypoglycemia arising from the pharmacological activity of exendin-4. Several approaches to reduce kidney uptake have been described in the literature, including pretargeting approaches [129] and other strategies to reduce nephrotoxicity [130] The first radioiodinated exendin-4 analogue to be developed to study and characterize exendin receptors was [^{125}I]-Tyr^{39}-exendin-4, where Ser^{39} has been replaced by Tyr^{39} for iodination [131]. The use of radiolabelled antagonists could well be a strategy to solve this issue with agonist-induced side effects. Moreover, as already found for other G-protein coupled receptors, radiolabelled antagonists could be more attractive as imaging agents due to higher tumor uptake and longer retention [78,132–135].

Studies from Goke et al. demonstrated that both exendin-4 and truncated exendin-(9–39)NH$_2$ specifically interact with the GLP-1 receptor on insulinoma-derived cells and on lung membranes and identified exendin-(9–39)NH$_2$ as a potent and specific GLP-1 receptor antagonist [136].

Further studies revealed that exendin-(9–39)NH$_2$ labelled with ^{125}I at Lys^{27}, using the Bolton and Hunter (BH) method ([^{125}I]BH-Ex(9–39)NH$_2$), was an excellent GLP-1R radioligand able to identify human and rat GLP-1 receptors in normal and tumor tissues [137] Moreover, [^{125}I]BH-Ex(9–39)NH$_2$ also showed favourable biodistribution in Ins-1E-bearing mice, with tumor uptake comparable to that of [^{68}Ga]DOTA-exendin-4 ([Nle^{14},Lys^{40}(Ahx-DOTA-[^{68}Ga])NH$_2$]Ex-4), the PET tracer used for detection of insulinoma [138]. Remarkably, radioiodination led to a considerable decrease of kidney uptake. In comparison to [^{68}Ga]DOTA-exendin-4, the tumor-to-kidney ratio of [^{125}I]BH-Ex(9–39)NH$_2$ improved 20-fold suggesting that both ^{124}I- and ^{131}I-labelled congeners could be promising candidates for theranostic approaches [139].

Recently, a direct radiodination approach was also explored aiming to improve the pharmacokinetics of GLP-1 receptor ligands. Both the GLP-1R agonist [Nle^{14}, ^{125}I-Tyr^{40}-NH$_2$]Ex-4 and the antagonist [Nle^{14},[^{125}I]-Tyr^{40}-NH$_2$]Ex(9–39) were evaluated and compared with the clinical PET tracer [^{68}Ga]DOTA-exendin-4 [140]. Biodistribution studies in nude mice bearing Ins-1E xenografts have shown that the agonist [Nle^{14},[^{125}I]-Tyr^{40}-NH$_2$]Ex-4 presented a tumor uptake identical to that of [^{68}Ga]DOTA-exendin-4, but substantially lower kidney uptake resulting in a high tumor-to-kidney ratio (9.7), which was even better than the ratio reported (3.5) for the antagonist [^{125}I]BH-Ex(9–39)NH$_2$ [140]. Moreover, preclinical PET imaging data strongly suggested that [Nle^{14},[^{124}I]-Tyr^{40}-NH$_2$]Ex-4 might be a promising alternative to the radiometal labelled derivatives for imaging of GLP-1 receptor positive insulinoma (Fig. 12).

Liraglutide is an acylated GLP-1 analogue in which Lys^{34} of the natural GLP-1 molecule has been replaced by Arg, and Lys^{26} has

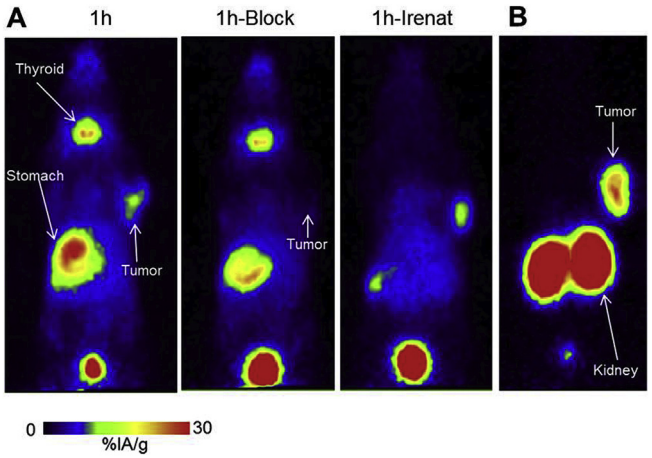

Fig. 12. PET images of [Nle^{14},[^{124}I]-Tyr^{40}-NH$_2$]Ex-4 (**A**) and [^{68}Ga]DOTA-exendin-4 (**B**). Biodistribution in Ins-1E tumor-bearing mice at 1 h post-injection. Middle panels show images of [Nle^{14},[^{124}I]-Tyr^{40}-NH$_2$]Ex-4 after blocking the non-specific uptake with Ex(9–39) and the sodium iodide symporter with irenat. Adapted from Lappchen et al. [140].

been modified by the addition of a C16 fatty acid (palmitic acid) with a glutamic acid spacer (Table 3) [141]. Consequently, liraglutide is not susceptible to degradation by DPP-IV while retaining the function of natural GLP-1. Liraglutide has been widely used for the clinical treatment of type 2 diabetes with good therapeutic effects.

A new, non-invasive imaging approach for the specific diagnosis of insulinoma was explored through initial examination of the use of ^{125}I-labelled liraglutide for small-animal SPECT/CT imaging of insulinomas [142]. The tumors could be visualized within 30 min after administration of the tracer and the clearest images were obtained at 90 min post-injection. Moreover, blocking experiments ascertained the radioligand specificity for GLP-1 receptors (Fig. 13).

2.5. Targeting the melanocortin 1 (MC1) receptor

α-Melanocyte-stimulating hormone (α-MSH, α-melanotropin) is a brain and pituitary 13-amino acid peptide that is mainly involved in the control of skin pigmentation [143]. The amino acid sequences of α-MSH and other linear α-MSH analogues are displayed in Table 4.

Five subtypes of melanocortin receptors (MC1R-MC5R), which belong to the superfamily of G protein-coupled receptors, have been cloned [144–146]. and references therein The overexpression of MC1R in more than 80% of human metastatic melanoma turned

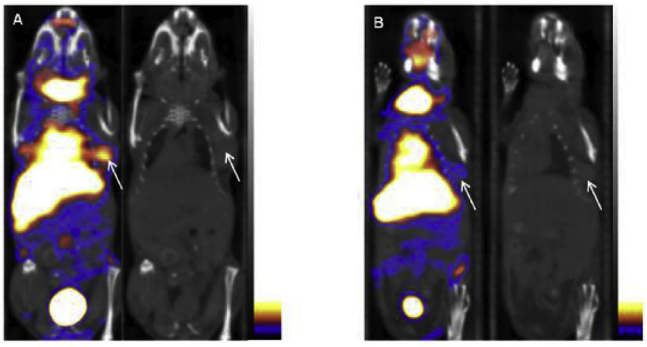

Fig. 13. SPECT/CT images of [^{125}I]liraglutide in the insulinoma model prior to blocking with liraglutide (**A**) and 90 min after blocking (**B**). The arrows indicate the tumor location. Adapted from Lv et al. [142].

Table 4
Schematic structures of linear α-MSH derivatives and of their radioiodinated analogues.

Amino acid sequence:
α-MSH
Ac-Ser^1-Tyr^2-Ser^3-Met^4-Glu^5-His^6-Phe^7-Arg^8-Trp^9-Gly^{10}-Lys^{11}-Pro^{12}-Val^{13}-NH$_2$
NDP-MSH
Ac-Ser-Tyr-Ser-**Nle^4**-Glu-His-**DPhe^7**-Arg-Trp-Gly-Lys-Pro-Val-NH$_2$
NAPamide
Ac-Nle^4-Asp-His-DPhe^7-Arg-Trp-Gly-Lys^{11}-NH$_2$
[^{125}I]-α-MSH
Ac-Ser-[^{125}I]Tyr^2-Ser-Met^4-Glu-His-Phe-Arg-Trp-Gly-Lys-Pro-Val-NH$_2$
[^{125}I]NDP-MSH
Ac-Ser^1-[^{125}I]Tyr^2-Ser-Nle^4-Glu-His-DPhe^7-Arg-Trp-Gly-Lys-Pro-Val-NH$_2$
[^{125}I]-3-iodobenzoate-NDP-MSH
Ac-Ser-Tyr-Ser-Nle^4-Glu-His-DPhe^7-Lys^{11}-3[^{125}I]IBA-Pro-Val-NH$_2$
[^{125}I]-4-iodobenzoate-NDP-MSH
Ac-Ser-Tyr-Ser-Nle^4-Glu-His-DPhe^7-Lys^{11}-4[^{125}I]IBA-Pro-Val-NH$_2$

IBA: iodobenzoic acid.

it into a potential relevant target for imaging and systemic radiotherapy [145]. In recent years, several radiolabelled α-MSH analogues have been explored as potential candidates for MC1R targeting and have been evaluated for both melanoma imaging and radionuclide therapy [147–151].

SAR studies have identified the amino acid sequence His-Phe-Arg-Trp as the minimal motif required for biological activity. Also, the replacement of Met^4 and Phe^7 by the synthetic amino acids Nle and DPhe, respectively, lead to a more potent analogue, [Nle^4,D-Phe^7]-α-MSH (NDP-MSH), which displayed higher MC1R binding affinity, longer half-life and increased enzymatic stability than the endogenous α-MSH [145]. The truncated linear NDP-MSH analogue [Ac-Nle^4,Asp^5,DPhe^7]-α-MSH$_{4-11}$ (NAPamide), designed by Froidevaux and colleagues, has been the most studied analogue for melanoma targeting *in vivo*.

The synthesis and application of several radioiodinated α-MSH analogues, including [^{125}I]-α-MSH, [^{125}I]-[Nle^4]-α-MSH and [^{125}I]-[Nle^4, DPhe^7]-α-MSH ([^{125}I] NDP-MSH), in receptor binding assays have been reported in the literature [42,44,152–157]. [^{125}I]NDP-MSH, the most widely used linear α-MSH peptide analogue, has been considered the "gold" standard due to its sub-nanomolar receptor binding affinity [158]. However, despite the excellent cell-binding characteristics *in vitro* [156], [^{125}I]NDP-MSH is prone to *in vivo* dehalogenation, which reduces its therapeutic potential and therefore restricts its application to *in vitro* studies [154].

In vivo deiodination has been largely overcame by labelling NDP-MSH with radioiodinated prosthetic groups, such as [^{125}I]SIB or [^{125}I]PIB [51,159]. The *in vitro* binding of [^{125}I]-3-iodobenzoate-NDP-MSH, labelled at Lys^{11} using [^{125}I]SIB, to a murine B-16 melanoma cell line was more than twice as high as that found for [^{131}I] NDP-MSH [159]. The inertness of this tracer to *in vivo* dehalogenation was demonstrated by the observation of decreased radioactivity in the thyroid and stomach of mice injected intravenously with [^{125}I]-3-iodobenzoate-NDP-MSH when compared to [^{131}I] NDP-MSH. However, biodistribution studies in melanoma-bearing mice have not been reported in the literature yet.

Likewise, NDP-MSH was radioiodinated with [^{125}I]PIB for biological investigation. *In vitro* receptor binding assays demonstrated that attachment of the 4-iodobenzoate group at Lys^{11} did not alter the peptide bioactivity. [51] In biodistribution studies carried out in a B16/F1 melanoma bearing mouse model [^{125}I]-4-iodobenzoate-NDP-MSH ([^{125}I]IBA-NDP-MSH) demonstrated a faster clearance from normal tissues and whole body as well as a higher tumor uptake and retention than NDP-MSH directly labelled with ^{125}I.

Since α-MSH analogues labelled with either radiohalogens or

radiometals are potential candidates for melanoma targeting, it is important to compare the biodistribution profiles of radiohalogenated (^{125}I-labelled) and radiometalated (^{111}In-labelled) α-MSH analogues. A comparison of [^{125}I]IBA-NDP-MSH with ^{111}In-DOTA-NDP-MSH suggested distinct profiles in B16/F1 murine melanoma bearing C57 BL/6 mice [51]. The tumor uptake for the ^{111}In-labelled peptide at 24 h *p.i.* was ca. 10-fold higher than that of the ^{125}I-labelled peptide even though its clearance from normal tissues was slower. Also, the uptake for the dose-limiting kidneys was significantly higher for [^{111}In]DOTA-NDP-MSH. The different metabolic patterns of radioiodinated versus radiometalated peptides could help to explain the observed biodistribution patterns. The catabolites arising from the iodinated peptide (*i.e.* [^{125}I]iodobenzoic acid and its lysine conjugate) are probably expelled from the cells and excreted faster from the body whereas the free radiometal and/or the radiometal chelate complex remain in the cells following to the metabolic process. This can lead to an apparent higher radioactivity accumulation in the kidneys [160–163]. Distinct clearance pathways were also exhibited by both ligands, with [^{125}I]IBA-NDP-MSH clearing through both the urinary and gastrointestinal tract and [^{111}In]DOTA-NDP-MSH clearing predominantly via the renal pathway.

Radioiodinated α-MSH analogues were re-investigated using the cyclic α-MSH analog ReO[Cys^{3,4,10}DPhe^{7}]-α-MSH$_{3-13}$ (ReCCMSH) (Fig. 14) as a structural motif for radioiodination since metal-promoted cyclization has shown to increase peptide stability and tumor retention. Lys and D-Lys were coupled to the N-terminus of Re(Arg^{11})CCMSH to yield Ac-Lys-Re(Arg^{11})CCMSH and Ac-DLys-Re(Arg^{11})CCMSH, respectively that were subsequently labelled with ^{125}I at Lys^{3} using the commercially available prosthetic group [^{125}I]PIB (Fig. 14) [51]. The high melanoma uptake and prolonged tumor retention of Ac-DLys([^{125}I]IBA)-Re(Arg^{11})CCMSH in B16/F1 melanoma tumor-bearing mice was comparable to [^{111}In]-DOTA-Re(Arg^{11})CCMSH [164], and could be attributed to both rhenium cyclization and DLys incorporation. The favourable *in vivo* biodistribution observed clearly highlighted the potential of Ac-DLys-Re(Arg^{11})CCMSH as an excellent candidate for additional imaging and therapeutic studies [51].

Although both Ac-DLys([^{125}I]IBA)-ReCCMSH(Arg^{11}) and Ac-Lys([^{125}I]IBA)-ReCCMSH(Arg^{11}) showed high tumor uptake at 4-h p.i. in mice bearing B16F1 tumors the observed overall high background organ activity accumulation has prevented their successful application in SPECT imaging. [51].

2.6. Targeting the gastrin-releasing (GPR) receptor

The amidated tetradecapeptide bombesin (BBN) was originally isolated and characterized from the skin of the European frogs *Bombina bombina* and *Bombina variegata* [165]. The 27-amino acid gastrin-releasing peptide (GRP) is the mammalian counterpart of bombesin and was isolated a few years later from the porcine stomach [166]. It has a very high homology to bombesin, sharing the same 7-amino acid sequence (Trp^{8}-Ala^{9}-Val^{10}-Gly^{11}-Hist^{12}-Leu^{13}-Met^{14}-NH$_2$) at the C-terminal, which is the biologically active part. Both peptides are biologically active in the central nervous system (CNS) and in peripheral tissues. Shortly thereafter a novel BBN-like decapeptide with a common C-terminal methionine amide was identified in porcine spinal cord [167]. The designation neuromedin B (NMB) was proposed for this peptide due to its involvement in the neural communication system of mammals as a neuromediator or hormone. The amino acid sequences of BBN, GRP and NMB are depicted in Table 5.

Four different bombesin receptor subtypes have been identified and characterized, namely the GRP receptor subtype (GRP-R or BB2), the neuromedin-B receptor subtype (NMB-R or BB1), the so-called orphan receptor subtype (BB3), and the BBN receptor subtype 4 (BB4) [152,168–171]. Their pharmacological activities include, among others, the stimulation of hormones releasing, such as gastrin and somatostatin. All four receptor subtypes are broadly distributed in the central nervous system as well as in the gastrointestinal tract. Three receptor subtypes (NMB-R, GRP-R and BB3) have shown to be expressed in variable degrees on a variety of tumors. GRP-R are the most frequently overexpressed receptors on human cancers, including breast (38–72%), pancreatic (75%), small cell lung (85–100%), non-small cell lung (74–78%), prostate (62–100%), head and neck squamous cell (100%) cancers and neuroblastomas/gliobastomas (72–85%) [82,172–175].

Several BBN analogues labelled with radiometals have been developed as diagnostic probes for SPECT [176–178] or for peptide receptor radionuclide therapy [179–182]. However, the first BBN derivatives to be prepared for preclinical applications were the radioiodinated analogues (Table 5). Leu^{4} in the bombesin scaffold was replaced by Tyr^{4}, and the resulting radioiodinated peptide. [^{125}I]-Tyr^{4}-BBN, prepared by an oxidative method using chloramine-T, has been used at first to identify BBN receptors expressed on the central nervous system and in normal human pancreatic membranes (Table 5) [183–185] Reversible, saturable, and specific binding was also found on several human cancer cell

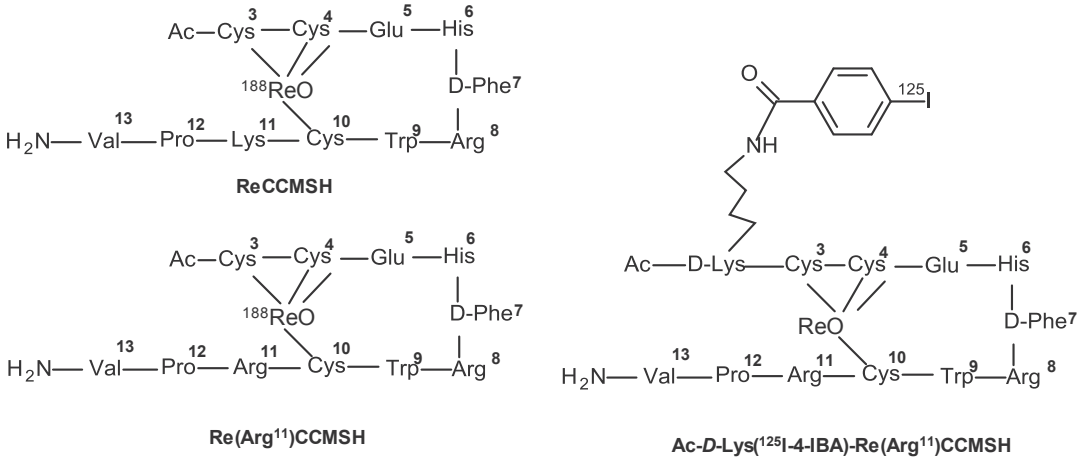

Fig. 14. Schematic structures of ReCCMSH, Re(Arg^{11})CCMSH and Ac-DLys([^{125}I]IBA)-Re(Arg^{11})CCMSH.

Table 5
Peptides targeting the gastrin-releasing peptide receptor (GRPR) and radioiodinated derivatives.

Amino acid sequence:
Bombesin (BBN)
*p*Glu^{1}-Gln^{2}-Arg^{3}-Leu^{4}-Gly^{5}-Asn^{6}-Gln^{7}-Trp^{8}-Ala^{9}-Val^{10}-Gly^{11}-Hist^{12}-Leu^{13}-Met^{14}-NH_2
GRP
Gly-Asn-His-Trp-Ala-Val-Gly-His-Leu-Met^{14}-NH_2
NMB
Gly-Asn-Leu-Trp-Ala-Thr-Gly-His-Phe-Met^{14}-NH_2
[^{125}I]-Tyr^{4}-bombesin
*p*Glu-Gln-Arg-Tyr^{4}[^{125}I]-Gly-Asn-Gln-Trp-Ala-Val-Gly-His-Leu-Met-NH_2
[DPhe^{6}, βAla^{11}, Phe^{13}, Nle^{14}]bombesin(6–14)
[DPhe^{6}-Gln-Trp-Ala-Val-βAla^{11}-His-Phe^{13}-Nle^{14}-NH_2
[^{125}I]-[DTyr^{6}, βAla^{11}, Phe^{13}, Nle^{14}]bombesin(6–14)
[^{125}I]-DTyr^{6}-Gln-Trp-Ala-Val-βAla^{11}-His-Phe^{13}-Nle^{14}-NH_2
[^{125}I]-mIP-Des-Met^{14}]bombesin(7–13)

Gln-Trp-Ala-Val-Gly-His-Leu-NH_2
BBN, GRP and NMB *are related in sequence and share an amidated methionine at their carboxyl termini. The entire structures of the different peptides are shown except for GRP which has 27 amino acids and only the COOH terminal 14 amino acids are shown, which is the biologically active end.*
Amino acids are shown in the standard three letter code

lines such as pancreatic, small-cell lung and prostate PC-3 and DU-145 [183,186,187]. [^{125}I]-Tyr^{4}-BBN is still used nowadays as a reference tracer in competitive binding assays and other radiometric studies [188,189].

To better elucidate the pharmacology of the orphan receptor bombesin receptor subtype 3 (BB3 or BRS-3), which was poorly characterized particularly in regard to its distribution and function in human tissues, Jensen and colleagues developed a synthetic peptide [DPhe^{6}, β-Ala^{11}, Phe^{13}, Nle^{14}]bombesin(6–14) with high affinity for all subtypes of bombesin receptors [190,191]. The radioiodinated analogue, [[^{125}I]-DTyr^{6}, β-Ala^{11}, Phe^{13}, Nle^{14}]bombesin(6–14), was then used to evaluate the expression of the various receptor subtypes in a selection of human tumors of different origins by means of *in vitro* receptor autoradiography allowing, for the first time, to identify BB3 and NMB receptor proteins in primary human tumors [192].

Another radioiodination approach, developed by Rogers and colleagues for BBN analogues, consisted on the conjugation of *m*-iodo-benzoic acid to the terminal Gln^{7} of Des-Met^{14}-bombesin(7–13)NH_2 to yield [^{125}I]-mIP-Des-Met^{14}-bombesin(7–13)NH_2 ([^{125}I]-mIP-BBN) (Table 5) [193].

Aiming to demonstrate the feasibility of a novel approach for peptide imaging or systemic radiotherapy, which combines the use of radiolabeled peptides with the genetic induction of high affinity receptors on tumors, internalization and catabolism of [^{125}I]-mIP-BBN and [^{125}I]-Tyr^{4}-BBN were compared in a GRP-R positive cell line [193]. The recombinant adenoviral vector (AdCMVGRPr) was used to induce the expression of the GRP-R *in vitro* in the murine BNR-11 cells and the human carcinoma cell lines A427, HeLa and SKO-V3.ipl. In a live-cell binding assay [^{125}I]-mIP-BBN showed more favourable internalization properties than [^{125}I]-Tyr^{4}-BBN and better tumor localization in mice bearing SKOV3.ipl ovarian tumors.

2.7. Targeting the chemokine receptor 4 (CXCR4)

Chemokines are a group of small glycoproteins that regulate cell trafficking of leukocytes through interactions with cell surface receptors [194,195]. The chemokine receptor 4 (**CXCR4**) is a G-protein-coupled receptor (GPCR) consisting of 352 amino acids. The interaction between CXCR4 and its natural ligand, the stromal cell-derived factor-1 (SDF-1, also known as CXCL12), an extracellular 72 amino acid chemokine, is a natural regulatory process in the human body. However, **CXCR4** overexpression is also found on more than 70% of human solid tumors, including breast cancer, prostate cancer, B-cell lymphoma, neuroblastoma, melanoma, cervical adenocarcinoma, and glioma, among others, where it plays a crucial role in metastatic spread [196–198]. For this reason CXCR4 is an attractive target in oncology and its clinical application in diagnosis and therapy is gaining increasing interest.

SDF-1 could be a logical choice for CXCR4 imaging. However, recent reports provided evidence that it also binds to another seven transmembrane span receptor called CXCR7, which may well influence the outcome of an imaging experiment. [199] The commercially available radioiodinated version of SDF-1, [^{125}I]SDF-1, obtained by radiodination of Tyr^{7} and/or Tyr^{61}, is often used as a reference in ligand binding assays with new CXCR4 imaging agents. [^{125}I]SDF-1 has shown to bind CXCR4 present in the brain and in neuroblastoma cells. Visualization of receptors was achieved by autoradiographic studies [200].

Aiming to develop novel radioiodinated probes for imaging CXCR4-expressing tumors, Han and colleagues have synthesized radioiodinated derivatives of T140, an highly potent specific antagonist of CXCR4, with high binding affinity and *in vivo* stability [201]. The most interesting compound [^{125}I]IBA-Ac-TZ14011 (Fig. 15) has been prepared by conjugation of [^{125}I]SIB to DLys^{8} of Ac-TZ14011 [202]. Its biodistribution profile, determined in healthy mice, showed a relatively fast clearance from the blood, mainly via the kidneys. Further labelling of Ac-TZ14011 with ^{124}I or ^{123}I and evaluation in mice with induced tumors is still necessary to ascertain the clinical potential of this new radioiodinated T140 analogue for CXCR4 imaging.

A family of cyclic pentapetides, with improved metabolic stability and high CXCR4 antagonism, was developed in an effort to downsize the CXCR4 ligand T140 [203,204]. These peptides consisted of Gly and the four pharmacologically most important residues of the T140 peptide (Arg^{2}, Nal^{3}, Tyr^{5} and Arg^{14}), which are responsible for the strong antagonistic activity of T140 [205] The peptide with the highest CXCR4 affinity *cyclo*(Nal^{1}-Gly^{2}-DTyr^{3}-Arg^{4}-Arg^{5}), also known as CPCR4 or FC131, was selected for further assays and was radioiodinated on *D*-Tyr with ^{123}I, ^{124}I or ^{125}I [206–209] (Fig. 15). [^{124}I]FC131 was the first PET imaging probe for CXCR4 targeting in preclinical evaluation [206]. It displayed high accumulation in CXCR4-positive tumors in an animal model and high focal uptake in lung micrometastases. However, its relatively high lipophilicity was probably responsible for the increased uptake found in the liver and intestines, which hampered its applicability for whole-body CXCR4 imaging.

2.8. Recent applications of radioiodinated peptides

Although some of the radioiodinated peptide probes developed so far showed promising results in preclinical studies only a limited number among them have been translated into clinical trials. However, the acquired knowledge along with the progress in a variety of strategies and optimized protocols for efficient radioiodination of peptides led, in recent years, to the design and evaluation of novel radioiodinated peptides as potential tools for molecular imaging of diverse biochemical processes including angiogenesis, apoptosis and hypoxia among others. Table 6 summarizes some of the more relevant radioiodinated peptide-based probes that have been recently assessed.

aSeveral endothelial molecular markers of angiogenesis

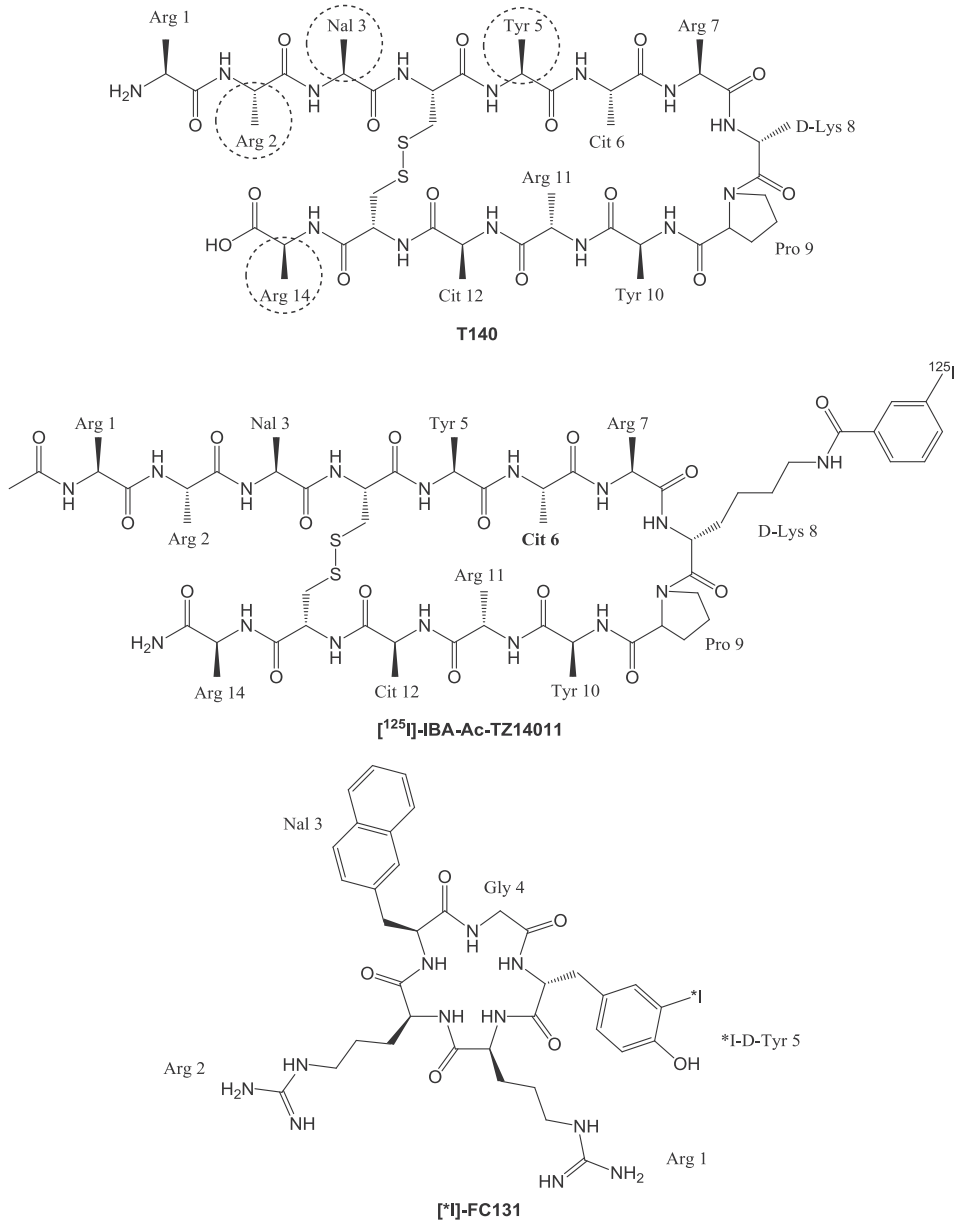

Fig. 15. Structure of T140 and its labelled analogue ^{125}I-labelled Ac-TZ14011 ([^{125}I]-IBA-Ac-TZ14011), and of the radioiodinated cyclopentapeptide [*I]-FC131 (*I = $^{123/or124/or125}$I). Nal = L-3-(2-naphthyl)alanine, Cit = L-citrulline. Circles identify the T140 residues that are indispensable for CXCR4-antagonistic activity.

expressed in tumor vasculature have been identified, including matrix metalloproteinases (MMPs), prostate specific membrane antigen (PSMA) and nucleolin, among others. In the last decade target-specific radioiodinated peptide-based tracers targeting some of those markers have been studied as nuclear imaging probes for non-invasive assessment of tumor angiogenesis.

MMPs are a family of zinc- and calcium-dependent membrane anchored endopeptidases that are responsible for degrading various extracellular matrix (ECM) components. MMP family includes five members, namely collagenases, gelatinases, stromolysins, membrane type-1 (MT1)-MMPs, and non-classified MMPs. A number of MMPs are specifically involved in angiogenesis, including gelatinases MMP2 and MMP9 that have been mostly associated with tumor aggressiveness and the development of metastases. *Cyclo*(-Cys-Thr-Thr-His-Trp-Gly-Phe-Thr-Leu-Cys) (CTT), a disulfide-bridged decapeptide, which selectively inhibits MMP2 and MMP 9, was identified using phage display libraries [217]. Imaging studies, carried out by the same researchers, showed the ability of its radioiodinated derivative Ala-Ala-[^{125}I]Tyr-*c*(Cys-Thr-Thr-His-Trp-Gly-Phe-Thr-Leu-Cys) ([^{125}I]AAYCTT) to localize tumors in mice bearing KS1767 Kaposi's sarcoma xenografts, suggesting its application in the early detection of primary tumors and metastasis [210]. Aimed at MT1-MMP targeting, Kondo and colleagues developed four radioiodinated peptide probes consisting of a MT1-MMP-specific binding sequence (L or D-amino acids) and an additional cysteine (at the N or C-terminus) for indirect labelling with [$^{123/125}$I]IPM (Table 6): [^{125}I]LN, [^{125}I]LC, [^{125}I]DN and [$^{123/125}$I]DC [211]. Among the probes evaluated in biodistribution studies in HT1080 tumor bearing mice, the D-amino acid-based peptides reached high tumor accumulation and a tumor/muscle ratio (3–5) comparable to that of MT1-MMP antibody-based imaging probes [218]. The fast blood clearance and the highest tumor/blood ratio achieved by [^{125}I]DC 10 min after injection suggested the potential of [^{123}I]DC for *in vivo* monitoring of MT1-MMP expression in cancers.

Table 6
Other recent radioiodinated peptide-based probes and respective targets.

Peptide	Amino acid sequence	Biomarker/ Target	Ref
[^{125}I]AAYCTT	Ala-Ala-[^{125}I]Tyr-c(Cys-Thr-Thr-His-Trp-Gly-Phe-Thr-Leu-Cys	MMP-	[210]
[^{125}I]LN	Ac-[^{125}IPM]Cys-Gly-His-Trp-Lys-His-Leu-His-Asn-Thr-Lys-Thr-Phe-Leu	2,MMP-9	[211]
[^{125}I]LC	Ac-His-Trp-Lys-His-Leu-His-Asn-Thr-Lys-Thr-Phe-Leu-[^{125}IPM]Cys	MT1-MMP	[211]
[^{125}I]DN	Ac-[^{125}IPM]DCys-Gly-DHis-DTrp-DLys-DHis-DLeu-DLeu-DHis-DAsn-DLys-DThr-DPhe-DLeu-DThr-DPhe-DLeu	MT1-MMP	[211]
[$^{125/123}$I]DC	Ac- DHis- DTrp-DLys- DHis-DLeu-DHis-DAsn-DLys-DThr-DPhe-DLeu-[$^{125/123}$IPM]-DCys	MT1-MMP	[211]
[^{125}I]BMF3	Lys-Asp-Glu-Pro-Gln-Arg-Arg-Ser-Ala-Arg-Leu-Ser Ala-Lys-Pro-Ala-Pro-Pro-Lys-Pro-Glu-Pro-Lys-Pro-Lys-Lys-Ala-Pro-Ala-Lys-Lys	MT1-MMP	[53]
[^{125}I]RRL	[^{125}IBM]Cys	Nucleolin	[212]
peptide	[^{131}I]Tyr-c(Cys-Gly-Gly-Arg-Arg-Leu-Gly-Gly-Cys)	Unknown	[213]
[^{125}I]cMBP[a]	Lys-Ser-Leu-Ser-Arg-His-Asp-His-Ile-His-His-His	c-Met	[213]
[^{125}I]cMBP-GGG*	Lys-Ser-Leu-Ser-Arg-His-Asp-His-Ile-His-His-Gly-Gly-Gly-Ser-Cys	c-Met	[213]
	Lys-Ser-Leu-Ser-Arg-His-Asp-His-Ile-His-His-His-AOC-Cys	c-Met	[214]
[^{125}I]	Ac-[$^{124/131}$I]Tyr-Cys-Gln-Arg-Pro-Pro-Arg-NH2	histone H1	[215]
cMBPAOC*	[^{125}I-IPM]Lys-Asn-Pro-Phe-Ser-Thr-Gln-Asp-Thr-Asp-Leu-Asp-Leu-Glu-Met-Leu-Ala-Pro-Tyr-Ile-Pro-Met-Asp-Asp-Asp-Phe-Gln-	HIF-1	[216]
[$^{124/131}$I]	Leu-Gly-Cys-NH2	HIF-1	[216]
ApoPep-1	[^{125}I-IPM]-Lys-Lys-Lys-Lys-Lys-Lys-Lys-Lys-Lys-Asp-Leu-Asp-Leu-Glu-Met-Leu-Ala-Pro-Tyr-Ile-Pro-Met-Asp-Asp-Asp-Phe-Gln-	HIF-1	[216]
[^{125}I]OP30	Leu-Gly-Cys-NH2	HIF-1	[216]
[^{125}I]KOP30	[^{125}I-IPM]-Lys-Lys-Lys-Lys-Lys-Lys-Lys-Lys-Lys-Asp-Leu-Asp-Leu-Glu-Met-Leu-Ala-Ala-Tyr-Ile-Ala-Met-Asp-Asp-Asp-Phe-Gln-		[216]
[^{125}I] mKOP	Leu-Gly-Cys-NH2		
[$^{123/125}$I]	[$^{123/125}$I-IPM]-DLys-DLys-DLys-DLys-DLys-DLys-DLys-DLys-DLys-Asp-Leu-Asp-Leu-Glu-Met-Leu-Ala-Pro-Tyr-Ile-Pro-Met-Asp-Asp-		
DKOP30	Asp-Phe-Gln-Leu-Gly-Cys-NH2		
[^{125}I]mDKOP	[$^{123/125}$I-IPM]-DLys-DLys-DLys-DLys-DLys-DLys-DLys-DLys-DLys-Asp-Leu-Asp-Leu-Glu-Met-Leu-Ala-Ala-Tyr-Ile-Ala-Met-Asp-Asp-		
	Asp-Phe-Gln-Leu-Gly-Cys-NH2		

IPM: N-(m-iodophenyl)maleimide; IBM: N-(2-aminoethyl)maleimide; AOC:8-aminooctanoic acid.
[a] the site of radioiodination has not been disclosed by the authors.

F3 peptide is a 31 amino acid fragment of HMGN2 protein identified by *in vivo* phage display techniques that has been shown to bind to tumor and endothelial cells in tumor blood vessels. [219] Subsequent research has identified nucleolin as the receptor/target for F3 peptide [220]. Nucleolin is a highly conserved nuclear protein ubiquitously distributed in the nucleolus, nucleus and cytoplasm of the cell, and that is primarily involved in rRNA synthesis and ribosome biogenesis [221,222]. It also acts as a shuttle protein transporting ribosomal proteins and subunits between the nucleus and the cytoplasm. A radioiodinated derivative of F3 peptide [^{125}I] IBMF3 was explored as a potential SPECT imaging agent in Van Dort's research group [53]. [^{125}I]IBMF3 was synthesized by incorporating a C-terminal cysteine residue for site-specific coupling to a radioiodinated maleimide conjugating group. SPECT imaging studies with [^{125}I]IBMF3 in nude mice bearing MDA-MB-435 xenografts showed a clear visualization of tumor following systemic administration. However, according to the authors, a structural modification of the tracer, such as the incorporation of a more hydrophilic linker for the attachment of the radionuclide, could possibly enhance the *in vivo* pharmacokinetics, reducing renal clearance and consequently increasing tumor uptake.

Using a peptide display library, Brown and colleagues identified various tumor vasculature−specific binding sequences, including the tumor endothelial cell-specific binding tripeptide Arg-Arg-Leu (RRL) [223]. A custom-synthesized 9-mer cyclic peptide *c*(Cys-Gly-Gly-Arg-Arg-Leu-Gly-Gly-Cys) containing the Arg-Arg-Leu sequence has been successfully used by Weller et al. to image tumor angiogenesis by ultrasonography and it was demonstrated that the peptide targeted tumor vasculature and is useful for *in vivo* detection of tumors [224]. Those promising results prompted its direct labelling with ^{131}I by incorporation of a N-terminal Tyr to allow iodination [212] yielding the radioiodinated analogue [^{131}I] RRL peptide. Biodistribution studies of the latter in nude mice bearing human prostate carcinoma (PC3) has shown high tumor uptake and good tumor to non-target organ ratios suggesting its clinical potential for visualization of tumors. However, the molecular target of this tumor-binding peptide has yet to be disclosed.

Another promising target for angiogenesis inhibition is the signaling pathway of hepatocyte growth factor (HGF) and its receptor (HGFR, also known as c-Met) [225]. C-Met, a receptor tyrosine kinase frequently observed in human glioblastomas, plays a pivotal role in angiogenesis and tumor growth. In a pioneer study by Kim et al., three ^{125}I-labelled c-Met binding peptides (cMBP) without any linker or with an amino acid Gly linker (Gly-Gly-Gly) or an 8-aminooctanoic acid linker (AOC) have been investigated as SPECT imaging probes to target c-Met-expressing tumors: [^{125}I]-cMBP, [^{125}I]-cMBP-GGG and [^{125}I]-cMBP-AOC [213]. Results from biodistribution studies revealed that the use of Gly residues increased tumor-to-blood ratio, with [^{125}I]-cMBP-Gly-Gly-Gly being clearly visualized in U87MG mice xenografts. However, according to the researchers these promising results can be potentially improved by structural modification of the linkers.

A novel histone H1 targeting peptide (Cys-Gln-Arg-Pro-Pro-Arg-NH_2), named Apoptosis-targeting Peptide-1 (ApoPep-1) was identified by Wang et al. using phage-display peptide libraries [214]. It was was devised as a promising probe for imaging apoptosis *in vivo* due to its ability to target apoptotic and necrotic cells by binding to histone H1 on the surface of apoptotic cells and in the nucleus of necrotic cells. The *in vivo* targeting ability of radioiodinated ApoPep-1 peptide ([$^{124/131}$I]ApoPep-1) was evaluated in various murine models of apoptosis. Biodistribution data and microPET imaging results clearly demonstrated the high potential of radioiodinated ApoPep-1 as an apoptosis specific imaging agent [215].

Hypoxia-Inducible Factor (HIF-1), a dimeric protein complex expressed in *hypoxic* regions, plays important role in the body's response to low oxygen concentrations. In particular, the oxygen-dependent degradation domain (ODD) of HIF-1α is responsible for the regulation of HIF-1 activity. Thus, imaging of HIF-1-active regions in hypoxic tumor regions could provide valuable information for appropriate cancer therapy. Aiming to vizualise HIF-1α tumors, Ueda et al. have synthesized and evaluated five peptide imaging probes based on the degradation mechanism of HIF-1α [216]. The dipeptide Gly-Cys was conjugated to the C-terminal of the $ODD_{547-574}$ scaffold for site-specific radioiodination and the whole sequence was named OP30. Aiming to increase membrane permeability, the nine amino acids at the N-terminal of OP30 were

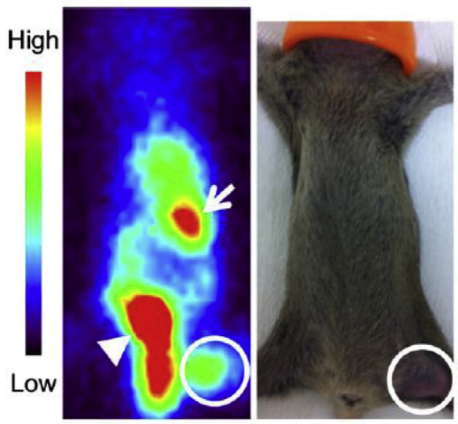

Fig. 16. A representative planar image of a FM3A-implanted mouse following administration of [^{123}I]DKOP30 (2 h). The tumor is clearly visualized in the image (circle). The gall bladder (arrow) and bladder (arrowhead) were also visible. Adapted with permission from Ueda et al. Copyrigth 2013 World Molecular Imaging Society [216].

replaced by Lys or D-Lys, providing KOP30 and DKOP30, respectively. Additionally, the Pro residues in KOP30 and DKOP30 that were essential to oxygen-dependent degradation of the peptides were replaced by L-Ala, giving mKOP and mDKOP, respectively. Radioiodination of all peptides was performed by an indirect method upon conjugating of the prosthetic group [$^{125/123}$I]IPM to the peptides. Among the ODD-based peptides that were evaluated, [^{123}I]DKOP30 emerged as the most useful probe for imaging HIF-1-active tumors. Biodistribution studies in FM3A mammary carcinoma-implanted mice showed tumoral accumulation of [^{125}I]DKOP30. Indeed, the tumor was clearly visualized after 2 h p.i. (Fig. 16), with intratumoral distribution correlating with the HIF-1α-positive hypoxic regions.

To address the clinical need for an imaging agent capable of detecting systemic amyloidosis, Wall and colleagues evaluated a series of seven radioiodinated heparin-binding peptides (p1-p7) (Table 7) by using small animal SPECT imaging, tissue biodistribution studies, and microautoradiography [226]. The radioiodinated 31-amino acid peptide [^{125}I]p5 bound specifically and selectively to murine serum amyloid protein A (AA) *in vivo*, suggesting its potential role as an amyloid non-invasive imaging agent for the rapid detection and monitoring of disease in patients with amyloidosis.

Following these promising results further studies were carried out with an Arg-substituted variant, p5R, in which the eight Lys amino acids of p5 have been replaced with Arg residues predisposing the peptide toward the α helical conformation [227]. The radioiodinated peptide, [^{125}I]p5R, showed higher affinity for amyloid and provided a clear visualization of AA amyloid in mice by using SPECT/CT imaging suggesting its potential for the *in vivo* detection of less dense and more vascular forms, as found in the brain and pancreatic vasculature.

Additionaly, the same researchers designed three variants of p5, ^{AQA}p5$_{(D)}$, ^{aqa}p5 and ^{AQA}p5 (Table 7), to study the effects of incorporating D-amino acids into amyloid-reactive peptides [228]. Following radioiodination these peptides exhibited distinct biodistribution and dehalogenation profiles in healthy mice. This study also evidenced that the incorporation of D-amino acids into the amyloid binding regions resulted in off-target binding in liver or kidneys while their placement at the N-terminus, such as in ^{aqa}p5, retained amyloid specificity and the improved resistance against deiodinases [229].

3. Concluding remarks and perspectives

Considerable efforts have been directed in recent years towards the development of radiolabeled peptides for tumor receptor imaging and targeted radionuclide therapy. Radiopeptides, including those labelled with radioiodine, continue to emerge as valuable tools for clinical and research investigations owing to their favourable pharmacokinetics and specific tumor targeting characteristics.

Iodine radioisotopes are attractive since they exhibit a wide range of nuclear properties suitable for various applications. ^{125}I has gained some special interest due to its readily availability and adequate nuclear characteristics. Indeed, ^{125}I-labelled tracers are commonly used in radiometric binding assays and many ^{125}I-labelled molecules are commercially available. Moreover, a ^{125}I-labelled compound can be a convenient tool for translating preclinical results up to humans since the replacement of ^{125}I with ^{123}I provides a labelled probe with suitable characteristics for SPECT imaging in humans. In addition, molecular imaging by PET can be achieved with the positron emitter ^{124}I and the translation to the radionuclide therapy using the β^-/γ emitter ^{131}I can also be easily accomplished.

Although some radioiodinated peptides have emerged in the last few years as promising new candidates for targeting various diseases [^{123}I]octreotide and [^{123}I]VIP were the only ones to reach a clinical trial. However, none of them has been approved as a radiopharmaceutical up to now. Further preclinical and clinical studies are still needed to address in more detail the molecular features that make radioiodinated peptides potentially useful tracers for imaging and radionuclide therapy.

Table 7
Radioiodinated amyloid-reactive peptides.

Peptide	Aminoacid sequence	Reference
[125I]p1	Cys-Gly-Gly-[^{125}I]Tyr-Ser-Ser-Ser-Arg-Pro-Val-Arg-Arg-Arg-Arg-Arg-Pro-Arg-Val-Ser-Arg-Arg-Arg-Arg-Arg-Gly-Gly-Arg-Arg-Arg-Arg	[226]
[125I]p2	Cys-Gly-Gly-[^{125}I]Tyr-Gly-Asp-Ala-Lys-Lys-Lys-Lys-Asp-Gly-Lys-Lys-Ala-Glu-Pro-Lys-Asn-Pro-Arg-Glu-Asn-Lys-Leu-Lys-Gln-Pro-GlyCys-Gly-	[227]
[125I]p3	Gly-[125I]Tyr-Gly-Pro-Lys-Lys-Gly-Ser-Lys-Lys-Ala-Val-Thr-Lys-Ala-Gln-Lys-Lys-Asp-Gly-Lys-Lys-Arg	[228]
[125I]p4	Cys-Gly-Gly-[^{125}I]Tyr-Ser-Arg-Pro-Arg-Ala-Arg-Ala-Arg-Ala-Arg-Asp-Gln-Thr-Leu	
[125I]p5	Cys-Gly-Gly-[^{125}I]Tyr-Ser-Lys-Ala-Gln-Lys-Ala-Gln-Ala-Lys-Gln-Lys-Ala-Gln-Lys-Ala-Gln-Ala-Gln-Lys-Ala-Gln-Ala-Lys-Gln-Ala-Lys-Gln	
[125I]p6	Cys-Gly-Gly-[^{125}I]Tyr-Pro-Arg-Arg-Arg-Arg-Ser-Ser-Ser-Arg-Pro-Ile-Arg-Arg-Arg-Arg-Pro-Arg-Arg-Ala-Ser-Arg-Arg	
[125I]p7	Cys-Gly-Gly-[^{125}I]Tyr-Phe-Ala-Lys-Leu-Asn-Cys-Arg-Leu-Tyr-Arg-Lys-Ala-Asn-Lys-Ser-Ser-Lys	
[125I]p5R	Gly-Gly-Gly-[^{125}I]Tyr-Ser-Arg-Ala-Gln-Arg-Ala-Gln-Ala-Arg-Gln-Arg-Arg-Gln-Ala-Gln-Arg-Ala-Gln-Arg-Ala-Gln-Ala-Arg-Gln-Ala-Arg-Gln	
[125I] AQAp5(D)	Ala-Gln-Ala-[^{125}I]DTyr-DSer-DLys-DAla-DGln-DLys-DAla-DGln-DAla-DLys-DGln-DLys-DAla-DGln-DLys-DAla-DGln-DAla-DGln-DLys-DAla-DGln-DAla-DLys-DGln	
[125I]aqap5	DAla-DGln-DAla-[^{125}I]Tyr-Ser-Lys-Ala-Gln-Lys-Ala-Gln-Ala-Lys-Gln-Lys-Ala-Gln-Lys-Ala-Gln-Ala-Gln-Lys-Ala-Gln-Ala-Lys-Gln-Ala-Lys-Gln	
[125I]AQAp5	Ala-Gln-Ala-[^{125}I]Tyr-Ser-Lys-Ala-Gln-Lys-Ala-Gln-Ala-Lys-Gln-Lys-Ala-Gln-Lys-Ala-Gln-Ala-Gln-Lys-Ala-Gln-Ala-Lys-Gln-Ala-Lys-Gln	

Acknowledgements

This work has been partially supported by the Fundação para a Ciência e a Tecnologia, Portugal, through the projects UID/Multi/04349/2019 and PTDC/QUI-NUC/30147/2017.

References

[1] I. Hamley, Small bioactive peptides for biomaterials design and therapeutics, Chem. Rev. 117 (2017) 14015–14041.
[2] D. Tesauro, A. Accardo, C. Diaferia, V. Milano, J. Guillon, L. Ronga, F. Rossi, Peptide-based drug-delivery systems in biotechnological applications: recent advances and perspectives, Molecules 24 (2019).
[3] L. Gentilucci, A. Tolomelli, F. Squassabia, Peptides and peptidomimetics in medicine, surgery and biotechnology, Curr. Med. Chem. 13 (2006) 2449–2466.
[4] J. Lau, M. Dunn, Therapeutic peptides: historical perspectives, current development trends, and future directions, Bioorg. Med. Chem. 26 (2018) 2700–2707.
[5] J. Correia, A. Paulo, P. Raposinho, I. Santos, Radiometallated peptides for molecular imaging and targeted therapy, Dalton Trans. 40 (2011) 6144–6167.
[6] I. Jackson, P. Scott, S. Thompson, Clinical applications of radiolabeled peptides for PET, Semin. Nucl. Med. 47 (2017) 493–523.
[7] C. Charron, J. Hickey, T. Nsiama, D. Cruickshank, W. Turnbull, L. Luyt, Molecular imaging probes derived from natural peptides, Nat. Prod. Rep. 33 (2016) 761–800.
[8] M. Opalinska, A. Hubalewska-Dydejczyk, A. Sowa-Staszczak, Radiolabeled peptides: current and new perspectives, Q. J. Nucl. Med. Mol. Imag. 61 (2017) 153–167.
[9] R.B. Firestone, E. Browne, Table of radioactive isotopes, Abstr. Pap. Am. Chem. Soc. 190 (1985) 98. NUL.
[10] D.-H. Kim, J.-H. Jung, S.H. Son, C.-Y. Kim, C.M. Hong, S.Y. Jeong, S.-W. Lee, J. Lee, B.-C. Ahn, Difference of clinical and radiological characteristics according to radioiodine avidity in pulmonary metastases of differentiated thyroid cancer, Nuclear medicine and molecular imaging 48 (2014) 55–62.
[11] J.R. Oh, B.C. Ahn, S.Y. Jeong, S.W. Lee, J. Lee, Radioiodine scan index: a simplified, quantitative treatment response parameter for metastatic thyroid carcinoma, Nuclear Medicine and Molecular Imaging 49 (2015) 174–181.
[12] D. Van Nostrand, The benefits and risks of I-131 therapy in patients with well-differentiated thyroid cancer, Thyroid 19 (2009) 1381–1391.
[13] M.K. Chen, M. Yasrebi, J. Samii, L.H. Staib, I. Doddamane, D.W. Cheng, The utility of I-123 pretherapy scan in I-131 radioiodine therapy for thyroid cancer, Thyroid 22 (2012) 304–309.
[14] R.H. Seevers, R.E. Counsell, Radioiodination techniques for small organic-molecules, Chem. Rev. 82 (1982) 575–590.
[15] D.S. Wilbur, Radiohalogenation of proteins - an overview of radionuclides, labeling methods, and reagents for conjugate labeling, Bioconjug. Chem. 3 (1992) 433–470.
[16] R. Yan, E. El-Emir, V. Rajkumar, M. Robson, A.P. Jathoul, R.B. Pedley, E. Arstad, One-pot synthesis of an I-125-Labeled trifunctional reagent for multiscale imaging with optical and nuclear techniques, Angew. Chem. Int. Ed. 50 (2011) 6793–6795.
[17] R. Yan, K. Sander, E. Galante, V. Rajkumar, A. Badar, M. Robson, E. El-Emir, M.F. Lythgoe, R.B. Pedley, E. Arstad, A one-pot three-component radiochemical reaction for rapid assembly of I-125-Labeled molecular probes, J. Am. Chem. Soc. 135 (2013) 703–709.
[18] A.A. Cant, S. Champion, R. Bhalla, S.L. Pimlott, A. Sutherland, Nickel-mediated radioiodination of aryl and heteroaryl bromides: rapid synthesis of tracers for SPECT imaging, Angew. Chem. Int. Ed. 52 (2013) 7829–7832.
[19] L. Koehler, K. Gagnon, S. McQuarrie, F. Wuest, Iodine-124: a promising positron emitter for organic PET chemistry, Molecules 15 (2010) 2686–2718.
[20] A.M.S. Braghirolli, W. Waissmann, J.B. da Silva, G.R. dos Santos, Production of iodine-124 and its applications in nuclear medicine, Appl. Radiat. Isot. 90 (2014) 138–148.
[21] G.L. Cascini, A.N. Asabella, A. Notaristefano, A. Restuccia, C. Ferrari, D. Rubini, C. Altini, G. Rubini, (124)Iodine: a longer-life positron emitter isotope-new opportunities in molecular imaging, BioMed Res. Int. (2014).
[22] V.V. Belov, A.A. Bonab, A.J. Fischman, M. Heartlein, P. Calias, M.I. Papisov, Iodine-124 as a label for pharmacological PET imaging, Mol. Pharm. 8 (2011) 736–747.
[23] G.B. Saha, Fundamentals of Nuclear Pharmacy, Springer-Verlag, New York, 1998.
[24] M. Breslav, A. McKinney, J.M. Becker, F. Naider, Preparation of radiolabeled peptides via an iodine exchange reaction, Anal. Biochem. 239 (1996) 213–217.
[25] J.C. Reubi, A somatostatin analog inhibits chondrosarcoma and insulinoma tumor-growth, Acta Endocrinol. 109 (1985) 108–114.
[26] E.P. Krenning, W.A.P. Breeman, P.P.M. Kooij, J.S. Lameris, W.H. Bakker, J.W. Koper, L. Ausema, J.C. Reubi, S.W.J. Lamberts, Localization of endocrine-related tumors with radioiodinated analog of somatostatin, Lancet 1 (1989) 242–244.
[27] E.P. Krenning, D.J. Kwekkeboom, W.H. Bakker, W.A.P. Breeman, P.P.M. Kooij, H.Y. Oei, M. Vanhagen, P.T.E. Postema, M. Dejong, J.C. Reubi, T.J. Visser, A.E.M. Reijs, L.J. Hofland, J.W. Koper, S.W.J. Lamberts, Somatostatin receptor scintigraphy with in-111-dtpa-D-phe(1) - and I-123-Tyr(3) -octreotide - the rotterdam experience with more than 1000 patients, Eur. J. Nucl. Med. 20 (1993) 716–731.
[28] R. Mikołajczak, H.R. Maecke, Radiopharmaceuticals for somatostatin receptor imaging, Nucl. Med. Rev. Cent. E Eur. *19* (2016) 126–132.
[29] B. Mock, Q.-H. Zheng, in: Robert E. Henkin (Ed.), Radiopharmaceutical Chemistry: Iodination Techniques, second ed., Elsevier, 2006.
[30] M. Béhé, M. Gotthardt, T.M. Behr, Cell Biol. 4 (2006) 149–154.
[31] S. Mushtaq, J. Jeon, A. Shaheen, B.S. Jang, S.H. Park, Critical analysis of radioiodination techniques for micro and macro organic molecules, J. Radioanal. Nucl. Chem. 309 (2016) 859–889.
[32] J. Tantchou, W. Slaunwhite, Synthesis Of Iodohistamine-I-125-2 For Radioimmunoassay, Prep. Biochem. 9 (1979) 379–390.
[33] A. Glazer, F. Sanger, Iodination Of Chymotrypsinogen, Biochem. J. 90 (1964) 92–&.
[34] S. Katugampola, Z. Pallikaros, A. Davenport, [I-125-His(9)]-Ghrelin, a novel radioligand for localizing GHS orphan receptors in human and rat tissue; up-regulation of receptors with atherosclerosis, Br. J. Pharmacol. 134 (2001) 143–149.
[35] J. Leyris, T. Roux, E. Trinquet, P. Verdie, J. Fehrentz, N. Oueslati, S. Douzon, E. Bourrier, L. Lamarque, D. Gagne, J. Galleyrand, C. M'kadmi, J. Martinez, S. Mary, J. Baneres, J. Marie, Homogeneous time-resolved fluorescence-based assay to screen for ligands targeting the growth hormone secretagogue receptor type 1a, Anal. Biochem. 408 (2011) 253–262.
[36] M. Demeule, A. Regina, C. Che, J. Poirier, T. Nguyen, R. Gabathuler, J.P. Castaigne, R. Beliveau, Identification and design of peptides as a new drug delivery system for the brain, J. Pharmacol. Exp. Ther. 324 (2008) 1064–1072.
[37] A. Yamada, H. Yano, Y. Takao, T. Ono, T. Matsumoto, K. Itoh, Nonmutated self-antigen-derived cancer vaccine peptides elicit an IgE-independent but mast cell-dependent immediate-type skin reaction without systemic anaphylaxis, J. Immunol. 176 (2006) 857–863.
[38] S.M. Moerlein, W. Beyer, G. Stocklin, No-Carrier-Added radiobromination and radioiodination of aromatic rings using insitu generated peracetic-acid, Journal of the Chemical Society-Perkin Transactions 1 (1988) 779–786.
[39] Coenen , H. H., Mertens , John, Mazière , Bernard, Radioionidation Reactions for Pharmaceuticals, Compendium for Effective Synthesis Strategies. Springer Netherlands2006.
[40] J.J. Marchalonis, An enzymic method for trace iodination of immunoglobulins and other proteins, Biochem. J. 113 (1969) 299.
[41] H. Hosoda, M. Kojima, H. Matsuo, K. Kangawa, Ghrelin and des-acyl ghrelin: two major forms of rat ghrelin peptide in gastrointestinal tissue, Biochem. Biophys. Res. Commun. 279 (2000) 909–913.
[42] W. Siegrist, F. Solca, S. Stutz, L. Giuffre, S. Carrel, J. Girard, A.N. Eberle, Characterization of receptors for alpha-melanocyte-stimulating hormone on human-melanoma cells, Cancer Res. 49 (1989) 6352–6358.
[43] G. Muccioli, M. Papotti, V. Locatelli, E. Ghigo, R. Deghenghi, Binding of I-125-labeled ghrelin to membranes from human hypothalamus and pituitary gland, J. Endocrinol. Investig. 24 (2001) RC7–RC9.
[44] A.N. Eberle, V.J. Verin, F. Solca, W. Siegrist, C. Kuenlin, C. Bagutti, S. Stutz, J. Girard, Biologically-active monoiodinated alpha-msh derivatives for receptor-binding studies using human-melanoma cells, J. Recept. Res. 11 (1991) 311–322.
[45] W. Siegrist, S. Stutz, A. Eberle, Homologous and heterologous regulation of alpha-melanocyte-stimulating hormone receptors in human and mouse melanoma cell-lines, Cancer Res. 54 (1994) 2604–2610.
[46] W. Siegrist, D. Willard, W. Wilkison, A. Eberle, Agouti protein inhibits growth of B16 melanoma cells in vitro by acting through melanocortin receptors, Biochem. Biophys. Res. Commun. 218 (1996) 171–175.
[47] G. Kim, S.J. Weiss, R.L. Levine, Methionine oxidation and reduction in proteins, Biochim. Biophys. Acta Gen. Subj. 1840 (2014) 901–905.
[48] A.E. Bolton, W.M. Hunter, Labeling of proteins to high specific radioactivities by conjugation to a I-125-Containing acylating agent - application to radioimmunoassay, Biochem. J. 133 (1973) 529–538.
[49] G. Vaidyanathan, M.R. Zalutsky, Preparation of N-succinimidyl 3- *I iodobenzoate: an agent for the indirect radioiodination of proteins, Nat. Protoc. 1 (2006) 707–713.
[50] S. Garg, P.K. Garg, M.R. Zalutsky, N-succinimidyl 5-(trialkylstannyl)-3-pyridinecarboxylates - a new class of reagents for protein radioiodination, Bioconjug. Chem. 2 (1991) 50–56.
[51] Z. Cheng, J.Q. Chen, T.P. Quinn, S.S. Jurisson, Radioiodination of rhenium cyclized alpha-melanocyte-stimulating hormone resulting in enhanced radioactivity localization and retention in melanoma, Cancer Res. 64 (2004) 1411–1418.
[52] L. Khawli, A. Vandenabbeele, A. Kassis, N-(Meta-[I-125]Iodophenyl)Maleimide - an agent for high-yield radiolabeling of antibodies, Nucl. Med. Biol. 19 (1992) 289–295.
[53] M.S. Bhojani, R. Ranga, G.D. Luker, A. Rehemtulla, B.D. Ross, M.E. Van Dort, Synthesis and investigation of a radioiodinated F3 peptide analog as a SPECT tumor imaging radioligand, PLoS One 6 (2011).
[54] E.M.F. Billaud, A. Vidal, A. Vincenot, S. Besse, B. Bouchon, E. Debiton, E. Miot-Noirault, I. Miladi, L. Rbah-Vidal, P. Auzeloux, J.M. Chezal, Development and

preliminary evaluation of TFIB, a new bimodal prosthetic group for bioactive molecule labeling, ACS Med. Chem. Lett. 6 (2015) 168–172.
[55] S. Hamant, J. Mathieu, C. Morin, I. Trimcev, M. Vidal, The beta-iodoethoxyl group - a stable unit for radioiodination, Bioorg. Med. Chem. Lett 4 (1994) 1687–1690.
[56] L. Cavina, D. van der Born, P. Klaren, M. Feiters, O. Boerman, F. Rutjes, Design of radioiodinated pharmaceuticals: structural features affecting metabolic stability towards in vivo deiodination, Eur. J. Org. Chem. (2017) 3387–3414.
[57] A. Unden, K. Tatemoto, V. Mutt, T. Bartfai, Neuropeptide-Y receptor in the rat-brain, Eur. J. Biochem. 145 (1984) 525–530.
[58] E. Martin, S. Kennel, T. Richey, C. Wooliver, D. Osborne, A. Williams, A. Stuckey, J. Wall, Dynamic PET and SPECT imaging with radioiodinated, amyloid-reactive peptide p5 in mice: a positive role for peptide dehalogenation, Peptides 60 (2014) 63–70.
[59] A. EBERLE, W. HUBSCHER, Alpha-melanotropin labeled at its tyrosine 2 residue - synthesis and biological-activities of 3'-iodotyrosine 2, 3'-I-125-Odotyrosine 2, 3',5'-diiodotyrosine 2, and (3',5'- (H2)-H-3)Tyrosine2-Alpha-Melanotropin, and of related peptides, Helv. Chim. Acta 62 (1979) 2460–2483.
[60] J.J. Miller, G.S. Schultz, R.S. Levy, Rapid purification of radioiodinated peptides with sep-pak reversed phase cartridges and hplc, Int. J. Pept. Protein Res. 24 (1984) 112–122.
[61] J.M. Conlon, Purification of naturally occurring peptides by reversed-phase HPLC, Nat. Protoc. 2 (2007) 191–197.
[62] D.F. Veber, F.W. Holly, R.F. Nutt, S.J. Bergstrand, S.F. Brady, R. Hirschmann, M.S. Glitzer, R. Saperstein, Highly-active cyclic and bicyclic somatostatin analogs of reduced ring size, Nature 280 (1979) 512–514.
[63] D.F. Veber, R.M. Freidinger, D.S. Perlow, W.J. Paleveda, F.W. Holly, R.G. Strachan, R.F. Nutt, B.H. Arison, C. Homnick, W.C. Randall, M.S. Glitzer, R. Saperstein, R. Hirschmann, A potent cyclic hexapeptide analog of somatostatin, Nature 292 (1981) 55–58.
[64] A. Kubota, Y. Yamada, S. Kagimoto, A. Shimatsu, M. Imamura, K. Tsuda, H. Imura, S. Seino, Y. Seino, Identification of somatostatin receptor subtypes and an implication for the efficacy of somatostatin analog sms-201-995 in treatment of human endocrine tumors, J. Clin. Investig. 93 (1994) 1321–1325.
[65] S.W.J. Lamberts, W.H. Bakker, J.C. Reubi, E.P. Krenning, Somatostatin-receptor imaging in the localization of endocrine tumors, N. Engl. J. Med. 323 (1990) 1246–1249.
[66] W.H. Bakker, E.P. Krenning, W.A. Breeman, P.P.M. Kooij, J.C. Reubi, J.W. Koper, M. Dejong, J.S. Lameris, T.J. Visser, S.W. Lamberts, Invivo use of a radioiodinated somatostatin analog - dynamics, metabolism, and binding to somatostatin receptor-positive tumors in man, J. Nucl. Med. 32 (1991) 1184–1189.
[67] R. Haubner, H.J. Wester, F. Burkhart, R. Senekowitsch-Schmidtke, W. Weber, S.L. Goodman, H. Kessler, M. Schwaiger, Glycosylated RGD-containing peptides, tracer for tumor targeting and angiogenesis imaging with improved biokinetics, J. Nucl. Med. 42 (2001) 326–336.
[68] R. Haubner, H.J. Wester, W.A. Weber, C. Mang, S.I. Ziegler, S.L. Goodman, R. Senekowitsch-Schmidtke, H. Kessler, M. Schwaiger, Noninvasive imaging of alpha(v)beta(3) integrin expression using F-18-labeled RGD-containing glycopeptide and positron emission tomography, Cancer Res. 61 (2001) 1781–1785.
[69] G. Vaidyanathan, H.S. Friedman, D.J. Affleck, M. Schottelius, H.J. Wester, M.R. Zalutsky, Specific and high-level targeting of radiolabeled octreotide analogues to human medulloblastoma xenografts, Clin. Cancer Res. 9 (2003) 1868–1876.
[70] M. Schottelius, R. Senekowitsch-Schmidtke, K. Scheidhauer, H. Kessler, M. Schwaiger, H.J. Wester, Glycated radioiodinated octreotides and octreotates with renal excretion and increased tumor uptake for SSTR scintigraphy and peptide receptor radionuclide therapy (PRRT), J. Nucl. Med. 41 (2000) 40P–41P.
[71] H.J. Wester, M. Schottelius, K. Scheidhauer, J.C. Reubi, I. Wolf, M. Schwaiger, Comparison of radioiodinated TOC, TOCA and Mtr-TOCA: the effect of carbohydration on the pharmacokinetics, Eur. J. Nucl. Med. 29 (2002) 28–38.
[72] A. Stahl, G. Meisetschlager, M. Schottelius, K. Bruus-Jensen, I. Wolf, K. Scheidhauer, M. Schwaiger, I-123 Mtr-TOCA, a radioiodinated and carbohydrated analogue of octreotide: scintigraphic comparison with In-111 octreotide, Eur. J. Nucl. Med. Mol. Imaging 33 (2006) 45–52.
[73] M. Schottelius, H.J. Wester, J.C. Reubi, R. Senekowitsch-Schmidtke, M. Schwaiger, Improvement of pharmacokinetics of radioiodinated Tyr(3)-octreotide by conjugation with carbohydrates, Bioconjug. Chem. 13 (2002) 1021–1030.
[74] M. Schottelius, F. Rau, J.C. Reubi, M. Schwaiger, H.J. Wester, Modulation of pharmacokinetics of radioiodinated sugar-conjugated somatostatin analogues by variation of peptide net charge and carbohydration chemistry, Bioconjug. Chem. 16 (2005) 429–437.
[75] G. Vaidyanathan, D. Affleck, P. Welsh, A. Srinavasan, M. Schmidt, M.R. Zalutsky, Radioiodination and astatination of octreotide by conjugation labeling, Nucl. Med. Biol. 27 (2000) 329–337.
[76] G. Vaidyanathan, A. Boskovitz, S. Shankar, M.R. Zalutsky, Radioiodine and At-211-labeled guanidinomethyl halobenzoyl octreotate conjugates: potential peptide radiotherapeutics for somatostatin receptor-positive cancers, Peptides 25 (2004) 2087–2097.
[77] G. Vaidyanathan, D.J. Affleck, M. Schottelius, H. Wester, H.S. Friedman, M.R. Zalutsky, Synthesis and evaluation of glycosylated octreotate analogues labeled with radioiodine and At-211 via a tin precursor, Bioconjug. Chem. 17 (2006) 195–203.
[78] D. Wild, M. Fani, M. Behe, I. Brink, J.E.F. Rivier, J.C. Reubi, H.R. Maecke, W.A. Weber, First clinical evidence that imaging with somatostatin receptor antagonists is feasible, J. Nucl. Med. 52 (2011) 1412–1417.
[79] J.C. Reubi, B. Waser, H. Macke, J. Rivier, Highly increased I-125-JR11 antagonist binding in vitro reveals novel indications for sst(2) targeting in human cancers, J. Nucl. Med. 58 (2017) 300–306.
[80] S.I. Said, V. Mutt, Polypeptide with broad biological activity - isolation from small intestine, Science 169 (1970) 1217–&.
[81] C.D. Ulrich, M. Holtmann, L.J. Miller, Secretin and vasoactive intestinal peptide receptors: members of a unique family of G protein-coupled receptors, Gastroenterology 114 (1998) 382–397.
[82] J.C. Reubi, Peptide receptors as molecular targets for cancer diagnosis and therapy, Endocr. Rev. 24 (2003) 389–427.
[83] I. Virgolini, Q. Yang, S.R. Li, P. Angelberger, N. Neuhold, B. Niederle, W. Scheithauer, P. Valent, Cross-competition between vasoactive-intestinal-peptide and somatostatin for binding to tumor-cell membrane-receptors, Cancer Res. 54 (1994) 690–700.
[84] I. Virgolini, M. Raderer, A. Kurtaran, P. Angelberger, S. Banyai, Q. Yang, S.R. Li, M. Banyai, J. Pidlich, B. Niederle, W. Scheithauer, P. Valent, Vasoactive intestinal peptide-receptor imaging for the localization of intestinal adenocarcinomas and endocrine tumors, N. Engl. J. Med. 331 (1994) 1116–1121.
[85] M. Raderer, A. Kurtaran, M. Hejna, F. Vorbeck, P. Angelberger, W. Scheithauer, I. Virgolini, I-123-labelled vasoactive intestinal peptide receptor scintigraphy in patients with colorectal cancer, Br. J. Canc. 78 (1998) 1–5.
[86] M. Raderer, A. Kurtaran, Q. Yang, S. Meghdadi, F. Vorbeck, M. Hejna, P. Angelberger, G. Kornek, J. Pidlich, W. Scheithauer, I. Virgolini, Iodine-123-vasoactive intestinal peptide receptor scanning in patients with pancreatic cancer, J. Nucl. Med. 39 (1998) 1570–1575.
[87] I. Virgolini, A. Kurtaran, M. Leimer, K. Kaserer, M. Peck-Radosavljevic, P. Angelberger, P. Hubsch, M. Dvorak, P. Valent, B. Niederle, Location of a VIPoma by iodine-123-vasoactive intestinal peptide scintigraphy, J. Nucl. Med. 39 (1998) 1575–1579.
[88] I. Virgolini, A. Kurtaran, M. Raderer, M. Leimer, P. Angelberger, E. Havlik, S.R. Li, W. Scheithauer, B. Niederle, P. Valent, H.G. Eichler, Vasoactive-intestinal-peptide receptor scintigraphy, J. Nucl. Med. 36 (1995) 1732–1739.
[89] I.D. Campbell, M.J. Humphries, Integrin structure, activation, and interactions, Cold Spring Harbor Perspect. Biol. 3 (2011).
[90] M. Barczyk, S. Carracedo, D. Gullberg, Integrins, Cell Tissue Res. 339 (2010) 269–280.
[91] D. Sheppard, Roles of alpha v integrins in vascular biology and pulmonary pathology, Curr. Opin. Cell Biol. 16 (2004) 552–557.
[92] E. Ruoslahti, M.D. Pierschbacher, New perspectives in cell-adhesion - rgd and integrins, Science 238 (1987) 491–497.
[93] J.P. Xiong, T. Stehle, R.G. Zhang, A. Joachimiak, M. Frech, S.L. Goodman, M.A. Arnaout, Crystal structure of the extracellular segment of integrin alpha V beta 3 in complex with an Arg-Gly-Asp ligand, Science 296 (2002) 151–155.
[94] M. Aumailley, M. Gurrath, G. Muller, J. Calvete, R. Timpl, H. Kessler, Arg-gly-asp constrained within cyclic pentapeptides - strong and selective inhibitors of cell-adhesion to vitronectin and laminin fragment-P1, FEBS Lett. 291 (1991) 50–54.
[95] M. Schottelius, B. Laufer, H. Kessler, H.J. Wester, Ligands for mapping alpha(v)beta(3)-Integrin expression in vivo, Acc. Chem. Res. 42 (2009) 969–980.
[96] S. Liu, Radiolabeled cyclic RGD peptides as integrin alpha(v)beta(3)-Targeted radiotracers: maximizing binding affinity via bivalency, Bioconjug. Chem. 20 (2009) 2199–2213.
[97] I. Dijkgraaf, A.J. Beer, H.J. Wester, Application of RGD-containing peptides as imaging probes for alphavbeta3 expression, Front. Biosci.-Landmark 14 (2009) 887–899.
[98] I. Dijkgraaf, O.C. Boerman, Molecular imaging of angiogenesis with SPECT, Eur. J. Nucl. Med. Mol. Imaging 37 (2010) S104–S113.
[99] R. Haubner, A.J. Beer, H. Wang, X.Y. Chen, Positron emission tomography tracers for imaging angiogenesis, Eur. J. Nucl. Med. Mol. Imaging 37 (2010) S86–S103.
[100] L.W. Dobrucki, E.D. de Muinck, J.R. Lindner, A.J. Sinusas, Approaches to multimodality imaging of angiogenesis, J. Nucl. Med. 51 (2010) 66S–79S.
[101] J. Shi, F. Wang, S. Liu, Radiolabeled cyclic RGD peptides as radiotracers for tumor imaging, Biophysics Reports 2 (2016) 1–20.
[102] M. Gurrath, G. Muller, H. Kessler, M. Aumailley, R. Timpl, Conformation activity studies of rationally designed potent antiadhesive rgd peptides, Eur. J. Biochem. 210 (1992) 911–921.
[103] R. Haubner, H.J. Wester, U. Reuning, R. Senekowitsch-Schmidtke, B. Diefenbach, H. Kessler, G. Stocklin, M. Schwaiger, Radiolabeled alpha(v)beta(3) integrin antagonists: a new class of tracers for tumor targeting, J. Nucl. Med. 40 (1999) 1061–1071.
[104] X.Y. Chen, R. Park, A.H. Shahinian, J.R. Bading, P.S. Conti, Pharmacokinetics and tumor retention of I-125-labeled RGD peptide are improved by PEGylation, Nucl. Med. Biol. 31 (2004) 11–19.
[105] R. Haubner, R. Gratias, B. Diefenbach, S.L. Goodman, A. Jonczyk, H. Kessler, Structural and functional aspects of RGD-containing cyclic pentapeptides as

highly potent and selective integrin alpha(v)beta(3) antagonists, J. Am. Chem. Soc. 118 (1996) 7461–7472.
[106] K. Ogawa, T. Takeda, K. Mishiro, A. Toyoshima, K. Shiba, T. Yoshimura, A. Shinohara, S. Kinuya, A. Odani, Radiotheranostics coupled between an at-211-labeled RGD peptide and the corresponding radioiodine-labeled RGD peptide, ACS Omega 4 (2019) 4584–4591.
[107] F. Haviv, T.D. Fitzpatrick, R.E. Swenson, C.J. Nichols, N.A. Mort, E.N. Bush, G. Diaz, G. Bammert, A. Nguyen, N.S. Rhutasel, H.N. Nellans, D.J. Hoffman, E.S. Johnson, J. Greer, Effect of N-methyl substitution of the peptide-bonds in luteinizing-hormone-releasing hormone agonists, J. Med. Chem. 36 (1993) 363–369.
[108] U. Wormser, R. Laufer, Y. Hart, M. Chorev, C. Gilon, Z. Selinger, Highly selective agonists for substance-P receptor subtypes, EMBO J. 5 (1986) 2805–2808.
[109] M.A. Dechantsreiter, E. Planker, B. Matha, E. Lohof, G. Holzemann, A. Jonczyk, S.L. Goodman, H. Kessler, N-methylated cyclic RGD peptides as highly active and selective alpha(v)beta(3) integrin antagonists, J. Med. Chem. 42 (1999) 3033–3040.
[110] N. Cini, A. Trabocchi, G. Menchi, A. Bottoncetti, S. Raspanti, A. Pupi, A. Guarna, Morpholine-based RGD-cyclopentapeptides as alpha(v)beta(3)/alpha(v)beta(5) integrin ligands: role of configuration towards receptor binding affinity, Bioorg. Med. Chem. 17 (2009) 1542–1549.
[111] F. Bianchini, N. Cini, A. Trabocchi, A. Bottoncetti, S. Raspanti, E. Vanzi, G. Menchi, A. Guarna, A. Pupi, L. Calorini, I-125-Radio labeled morpholine-containing arginine-glycine-aspartate (RGD) ligand of alpha(v)beta(3) integrin as a molecular imaging probe for angiogenesis, J. Med. Chem. 55 (2012) 5024–5033.
[112] A. Trabocchi, G. Menchi, N. Cini, F. Bianchini, S. Raspanti, A. Bottoncetti, A. Pupi, L. Calorini, A. Guarna, Click-chemistry-derived triazole ligands of arginine-glycine-aspartate (RGD) integrins with a broad capacity to inhibit adhesion of melanoma cells and both in vitro and in vivo angiogenesis, J. Med. Chem. 53 (2010) 7119–7128.
[113] F. Bianchini, P. Fabbrizzi, G. Menchi, S. Raspanti, A. Bottoncetti, A. Passeri, E. Andreucci, A. Guarna, L. Calorini, A. Pupi, A. Trabocchi, Radiosynthesis and micro-SPECT analysis of triazole-based RGD integrin ligands as non-peptide molecular imaging probes for angiogenesis, Bioorg. Med. Chem. 23 (2015) 1112–1122.
[114] M. Korner, M. Stockli, B. Waser, J.C. Reubi, GLP-1 receptor expression in human tumors and human normal tissues: potential for in vivo targeting, J. Nucl. Med. 48 (2007) 736–743.
[115] S. Mojsov, G. Heinrich, I.B. Wilson, M. Ravazzola, L. Orci, J.F. Habener, Preproglucagon gene-expression in pancreas and intestine diversifies at the level of posttranslational processing, J. Biol. Chem. 261 (1986) 1880–1889.
[116] D. Donnelly, The structure and function of the glucagon-like peptide-1 receptor and its ligands, Br. J. Pharmacol. 166 (2012) 27–41.
[117] M. Gotthardt, M. Fischer, I. Naeher, J.B. Holz, H. Jungclas, H.W. Fritsch, M. Behe, B. Goke, K. Joseph, T.M. Behr, Use of the incretin hormone glucagon-like peptide-1 (GLP-1) for the detection of insulinomas: initial experimental results, Eur. J. Nucl. Med. Mol. Imaging 29 (2002) 597–606.
[118] J. Eng, P.C. Andrews, W.A. Kleinman, L. Singh, J.P. Raufman, Purification and structure of exendin-3, a new pancreatic secretagogue isolated from heloderma-horridum venom, J. Biol. Chem. 265 (1990) 20259–20262.
[119] J. Eng, W.A. Kleinman, L. Singh, G. Singh, J.P. Raufman, Isolation and characterization of exendin-4, an exendin-3 analog, from heloderma-suspectum venom - further evidence for an exendin receptor on dispersed acini from Guinea-pig pancreas, J. Biol. Chem. 267 (1992) 7402–7405.
[120] D. Wild, H. Macke, E. Christ, B. Gloor, J.C. Reubi, Glucagon-like peptide 1-receptor scans to localize occult insulinomas, N. Engl. J. Med. 359 (2008) 766–768.
[121] D. Wild, A. Wicki, R. Mansi, M. Behe, B. Keil, P. Bernhardt, G. Christofori, P.J. Ell, H.R. Macke, Exendin-4-Based radiopharmaceuticals for glucagonlike peptide-1 receptor PET/CT and SPECT/CT, J. Nucl. Med. 51 (2010) 1059–1067.
[122] E. Christ, D. Wild, F. Forrer, M. Brandle, R. Sahli, T. Clerici, B. Gloor, F. Martius, H. Maecke, J.C. Reubi, Glucagon-like peptide-1 receptor imaging for localization of insulinomas, J. Clin. Endocrinol. Metab. 94 (2009) 4398–4405.
[123] A. Sowa-Staszczak, D. Pach, R. Mikolajczak, H. Macke, A. Jabrocka-Hybel, A. Stefanska, M. Tomaszuk, B. Janota, A. Gilis-Januszewska, M. Malecki, G. Kaminski, A. Kowalska, J. Kulig, A. Matyja, C. Osuch, A. Hubalewska-Dydejczyk, Glucagon-like peptide-1 receptor imaging with Lys(40)(Ahx-HYNIC-Tc-99m/EDDA)NH2 -exendin-4 for the detection of insulinoma, Eur. J. Nucl. Med. Mol. Imaging 40 (2013) 524–531.
[124] A. Sowa-Staszczak, M. Trofimiuk-Muldner, A. Stefanska, M. Tomaszuk, M. Buziak-Bereza, A. Gilis-Januszewska, A. Jabrocka-Hybel, B. Glowa, M. Malecki, T. Bednarczuk, G. Kaminski, A. Kowalska, R. Mikolajczak, B. Janota, A. Hubalewska-Dydejczyk, Tc-99m labeled glucagon-like peptide-1-analogue (Tc-99m-GLP1) scintigraphy in the management of patients with occult insulinoma, PLoS One 11 (2016).
[125] M. Brom, W.J.G. Oyen, L. Joosten, M. Gotthardt, O.C. Boerman, Ga-68-labelled exendin-3, a new agent for the detection of insulinomas with PET, Eur. J. Nucl. Med. Mol. Imaging 37 (2010) 1345–1355.
[126] N. Bandara, A. Zheleznyak, K. Cherukuri, D.A. Griffith, C. Limberakis, D.A. Tess, J.Q. Chen, R. Waterhouse, S.E. Lapi, Evaluation of Cu-64 and Ga-68 radiolabeled glucagon-like peptide-1 receptor agonists as PET tracers for pancreatic beta cell imaging, Mol. Imaging Biol. 18 (2016) 90–98.
[127] D.O. Kiesewetter, H.K. Gao, Y. Ma, G. Niu, Q.M. Quan, N. Guo, X.Y. Chen, F-18-radiolabeled analogs of exendin-4 for PET imaging of GLP-1 in insulinoma, Eur. J. Nucl. Med. Mol. Imaging 39 (2012) 463–473.
[128] Y.P. Xu, D.H. Pan, Q. Xu, C. Zhu, L.Z. Wang, F. Chen, R.L. Yang, S.N. Luo, M. Yang, Insulinoma imaging with glucagon-like peptide-1 receptor targeting probe F-18-FBEM-Cys(39)-exendin-4, J. Cancer Res. Clin. Oncol. 140 (2014) 1479–1488.
[129] S.M.J. van Duijnhoven, R. Rossin, S.M. van den Bosch, M.P. Wheatcroft, P.J. Hudson, M.S. Robillard, Diabody pretargeting with click chemistry in vivo, J. Nucl. Med. 56 (2015) 1422–1428.
[130] E. Vegt, M. de Jong, J.F.M. Wetzels, R. Masereeuw, M. Melis, W.J.G. Oyen, M. Gotthardt, O.C. Boerman, Renal toxicity of radiolabeled peptides and antibody fragments: mechanisms, impact on radionuclide therapy, and strategies for prevention, J. Nucl. Med. 51 (2010) 1049–1058.
[131] G. Singh, J. Eng, J.P. Raufman, Use of I-125 Y-39 exendin-4 to characterize exendin receptors on dispersed pancreatic acini and gastric chief cells from Guinea-pig, Regul. Pept. 53 (1994) 47–59.
[132] R. Cescato, T. Maina, B. Nock, A. Nikolopoulou, D. Charalambidis, V. Piccand, J.C. Reubi, Bombesin receptor antagonists may be preferable to agonists for tumor targeting, J. Nucl. Med. 49 (2008) 318–326.
[133] M. Ginj, H.W. Zhang, B. Waser, R. Cescato, D. Wild, X.J. Wang, J. Erchegyi, J. Rivier, H.R. Macke, J.C. Reubi, Radiolabeled somatostatin receptor antagonists are preferable to agonists for in vivo peptide receptor targeting of tumors, Proc. Natl. Acad. Sci. U. S. A 103 (2006) 16436–16441.
[134] K. Abiraj, R. Mansi, M.L. Tamma, M. Fani, F. Forrer, G. Nicolas, R. Cescato, J.C. Reubi, H.R. Maecke, Bombesin antagonist-based radioligands for translational nuclear imaging of gastrin-releasing peptide receptor-positive tumors, J. Nucl. Med. 52 (2011) 1970–1978.
[135] G. Wieser, R. Mansi, A.L. Grosu, W. Schultze-Seemann, R.A. Dumont-Walter, P.T. Meyer, H.R. Maecke, J.C. Reubi, W.A. Weber, Positron emission tomography (PET) imaging of prostate cancer with a gastrin releasing peptide receptor antagonist - from mice to men, Theranostics 4 (2014) 412–419.
[136] R. Goke, H.C. Fehmann, T. Linn, H. Schmidt, M. Krause, J. Eng, B. Goke, Exendin-4 is a high potency agonist and truncated exendin-(9-39)-amide an antagonist at the glucagon-like peptide 1-(7-36)-amide receptor of insulin-secreting beta-cells, J. Biol. Chem. 268 (1993) 19650–19655.
[137] B. Waser, J.C. Reubi, Radiolabelled GLP-1 receptor antagonist binds to GLP-1 receptor-expressing human tissues, Eur. J. Nucl. Med. Mol. Imaging 41 (2014) 1166–1171.
[138] K. Antwi, M. Fani, G. Nicolas, C. Rottenburger, T. Heye, J.C. Reubi, B. Gloor, E. Christ, D. Wild, Localization of hidden insulinomas with Ga-68-DOTA-Exendin-4 PET/CT: a pilot study, J. Nucl. Med. 56 (2015) 1075–1078.
[139] S.N. Rylova, B. Waser, L. Del Pozzo, R. Tonnesmann, R. Mansi, P.T. Meyer, J.C. Reubi, H.R. Maecke, Approaches to improve the pharmacokinetics of radiolabeled glucagon-like peptide-1 receptor ligands using antagonistic tracers, J. Nucl. Med. 57 (2016) 1282–1288.
[140] T. Lappchen, R. Tonnesmann, J. Eersels, P.T. Meyer, H.R. Maecke, S.N. Rylova, Radioiodinated exendin-4 is superior to the radiometal-labelled glucagon-like peptide-1 receptor probes overcoming their high kidney uptake, PLoS One 12 (2017).
[141] T. Vilsboll, Liraglutide: a once-daily GLP-1 analogue for the treatment of Type 2 diabetes mellitus, Expert Opin. Investig. Drugs 16 (2007) 231–237.
[142] J. Lv, Y. Pan, X. Li, D.F. Cheng, S. Liu, H.C. Shi, Y.F. Zhang, The imaging of insulinomas using a radionuclide-labelled molecule of the GLP-1 analogue liraglutide: a new application of liraglutide, PLoS One 9 (2014).
[143] R.D. Cone, K.G. Mountjoy, L.S. Robbins, J.H. Nadeau, K.R. Johnson, L. Rosellirehfuss, M.T. Mortrud, Cloning and functional-characterization of a family of receptors for the melanotropic peptides, Ann. N. Y. Acad. Sci. 680 (1993) 342–363.
[144] W. Siegrist, A.N. Eberle, Melanocortins and their implication in melanoma, Trends Endocrinol. Metabol. 6 (1995) 115–120.
[145] J.R. Holder, C. Haskell-Luevano, Melanocortin ligands: 30 years of structure-activity relationship (SAR) studies, Med. Res. Rev. 24 (2004) 325–356.
[146] Y.K. Yang, Structure, function and regulation of the melanocortin receptors, Eur. J. Pharmacol. 660 (2011) 125–130.
[147] P.D. Raposinho, J.D. Correia, M.C. Oliveira, I. Santos, Melanocortin-1 receptor-targeting with radiolabeled cyclic α-melanocyte-stimulating hormone analogs for melanoma imaging, Biopolymers 94 (2010) 820–829.
[148] Y.B. Miao, K. Benwell, T.P. Quinn, 99)mTc and In-111-labeled alpha-melanocyte-stimulating hormone peptides as imaging probes for primary and pulmonary metastatic melanoma detection, J. Nucl. Med. 48 (2007) 73–80.
[149] L.H. Wei, C. Butcher, Y.B. Miao, F. Gallazzi, T.P. Quinn, M.J. Welch, J.S. Lewis, Synthesis and biologic evaluation of Cu-64-labeled rhenium-cyclized alpha-MSH peptide analog using a cross-bridged cyclam chelator, J. Nucl. Med. 48 (2007) 64–72.
[150] L. Wei, Y. Miao, F. Gallazzi, T.P. Quinn, M.J. Welch, A.L. Vavere, J.S. Lewis, Gallium-68-labeled DOTA-rhenium-cyclized alpha-melanocyte-stimulating hormone analog for imaging of malignant melanoma, Nucl. Med. Biol. 34 (2007) 945–953.
[151] S. Froidevaux, M. Calame-Christe, H. Tanner, A.N. Eberle, Melanoma targeting with DOTA-alpha-melanocyte-stimulating hormone analogs: structural parameters affecting tumor uptake and kidney uptake, J. Nucl. Med. 46 (2005) 887–895.
[152] J.B. Tatro, M. Atkins, J.W. Mier, S. Hardarson, H. Wolfe, T. Smith,

M.L. Entwistle, S. Reichlin, Melanotropin receptors demonstrated insitu in human-melanoma, J. Clin. Investig. 85 (1990) 1825–1832.
[153] J.B. Tatro, S. Reichlin, Specific receptors for alpha-melanocyte-stimulating hormone are widely distributed in tissues of rodents, Endocrinology 121 (1987) 1900–1907.
[154] A.N. Eberle, S. Froidevaux, Radiolabeled alpha-melanocyte-stimulating hormone analogs for receptor-mediated targeting of melanoma: from tritium to indium, J. Mol. Recognit. 16 (2003) 248–254.
[155] W. Siegrist, C. Bagutti, F. Solca, J. Girard, A.N. Eberle, Msh receptors on mouse and human-melanoma cells - receptor identification, analysis and quantification, Prog. Histochem. Cytochem. 26 (1992) 110–118.
[156] W. Siegrist, M. Oestreicher, S. Stutz, J. Girard, A.N. Eberle, Radioreceptor assay for alpha-msh using mouse B-16 melanoma-cells, J. Recept. Res. 8 (1988) 323–343.
[157] W. Lichtensteiger, B. Hanimann, M. Schlumpf, W. Siegrist, A.N. Eberle, Prenatal and postnatal ontogeny of I-125 nle(4),d-phe(7)-alpha-msh binding-sites in rat-brain, Ann. N. Y. Acad. Sci. 680 (1993) 652–654.
[158] J.Q. Chen, Z. Cheng, T.J. Hoffman, S.S. Jurisson, T.P. Quinn, Melanoma-targeting properties of (99m)technetium-labeled cyclic alpha-melanocyte-stimulating hormone peptide analogues, Cancer Res. 60 (2000) 5649–5658.
[159] P.K. Garg, K.L. Alston, P.C. Welsh, M.R. Zalutsky, Enhanced binding and inertness to dehalogenation of alpha-melanotropic peptides labeled using N-succinimidyl 3-iodobenzoate, Bioconjug. Chem. 7 (1996) 233–239.
[160] F. Geissler, S.K. Anderson, P. Venkatesan, O. Press, Intracellular catabolism of radiolabeled anti-mu antibodies by malignant B-cells, Cancer Res. 52 (1992) 2907–2915.
[161] J.H. Labadie, K.P. Chapman, N.N. Aronson, Glycoprotein catabolism in rat-liver - lysosomal digestion of iodinated asialo-fetuin, Biochem. J. 152 (1975) 271–279.
[162] H. Sands, P.L. Jones, Methods for the study of the metabolism of radiolabeled monoclonal-antibodies by liver and tumor, J. Nucl. Med. 28 (1987) 390–398.
[163] L.B. Shih, S.R. Thorpe, G.L. Griffiths, H. Diril, G.L. Ong, H.J. Hansen, D.M. Goldenberg, M.J. Mattes, The processing and fate of antibodies and their radiolabels bound to the surface of tumor-cells in-vitro - a comparison of 9 radiolabels, J. Nucl. Med. 35 (1994) 899–908.
[164] Z. Cheng, J.Q. Chen, Y. Miao, N.K. Owen, T.P. Quinn, S.S. Jurisson, Modification of the structure of a metallopeptide: synthesis and biological evaluation of (111)in-labeled DOTA-conjugated rhenium-cyclized alpha-MSH analogues (vol 45, pg 3051, 2002), J. Med. Chem. 45 (2002), 4588-4588.
[165] A. Anastasi, V. Erspamer, M. Bucci, Isolation and structure of bombesin and Alytesin, 2 analogous active peptides from skin of european Amphibians Bombina and Alytes, Experientia 27 (1971) 166–&.
[166] T.J. McDonald, H. Jornvall, G. Nilsson, M. Vagne, M. Ghatei, S.R. Bloom, V. Mutt, Characterization of a gastrin releasing peptide from porcine non-antral gastric tissue, Biochem. Biophys. Res. Commun. 90 (1979) 227–233.
[167] N. Minamino, K. Kangawa, H. Matsuo, Neuromedin-B - a novel bombesin-like peptide identified in porcine spinal-cord, Biochem. Biophys. Res. Commun. 114 (1983) 541–548.
[168] E.R. Spindel, E. Giladi, P. Brehm, R.H. Goodman, T.P. Segerson, Cloning and functional-characterization of a complementary-dna encoding the murine fibroblast bombesin gastrin-releasing peptide receptor, Mol. Endocrinol. 4 (1990) 1956–1963.
[169] E. Wada, J. Way, H. Shapira, K. Kusano, A.M. Lebacqverheyden, D. Coy, R. Jensen, J. Battey, Cdna cloning, characterization, and brain region specific expression of a neuromedin-B preferring bombesin receptor, Neuron 6 (1991) 421–430.
[170] Z. Fathi, M.H. Corjay, H. Shapira, E. Wada, R. Benya, R. Jensen, J. Viallet, E.A. Sausville, J.F. Battey, Brs-3 - a novel bombesin receptor subtype selectively expressed in testis and lung-carcinoma cells, J. Biol. Chem. 268 (1993) 5979–5984.
[171] S.R. Nagalla, B.J. Barry, K.C. Creswick, P. Eden, J.T. Taylor, E.R. Spindel, Cloning of a receptor for Amphibian phe(13) bombesin distinct from the receptor for gastrin-releasing peptide - identification of a 4th bombesin receptor subtype (Bb4), Proc. Natl. Acad. Sci. U. S. A 92 (1995) 6205–6209.
[172] R.T. Jensen, J.F. Battey, E.R. Spindel, R.V. Benya, International union of pharmacology. LXVIII. Mammalian bombesin receptors: nomenclature, distribution, pharmacology, signaling, and functions in normal and disease states, Pharmacol. Rev. 60 (2008) 1–42.
[173] O. Patel, A. Shulkes, G.S. Baldwin, Gastrin-releasing peptide and cancer, Biochim. Biophys. Acta Rev. Canc. 1766 (2006) 23–41.
[174] N. Gonzalez, T.W. Moody, H. Igarashi, T. Ito, R.T. Jensen, Bombesin-related peptides and their receptors: recent advances in their role in physiology and disease states, Curr. Opin. Endocrinol. Diabetes Obes. 15 (2008) 58–64.
[175] H. Ohki-Hamazaki, M. Iwabuchi, F. Maekawa, Development and function of bombesin-like peptides and their receptors, Int. J. Dev. Biol. 49 (2005) 293–300.
[176] A. Varvarigou, P. Bouziotis, C. Zikos, F. Scopinaro, G. De Vincentis, Gastrin-releasing peptide (GRP) analogues for cancer imaging, Cancer Biother. Radiopharm. 19 (2004) 219–229.
[177] C.D. Ferreira, L.L. Fuscaldi, D.M. Townsend, D. Rubello, A.L.B. de Barros, Radiolabeled bombesin derivatives for preclinical oncological imaging, Biomed. Pharmacother. 87 (2017) 58–72.
[178] I. Ramos-Alvarez, P. Moreno, S.A. Mantey, T. Nakamura, B. Nuche-Berenguer, T.W. Moody, D.H. Coy, R.T. Jensen, Insights into bombesin receptors and ligands: highlighting recent advances, Peptides 72 (2015) 128–144.
[179] H.W. Zhang, J.H. Chen, C. Waldherr, K. Hinni, B. Waser, J.C. Reubi, H.R. Maecke, Synthesis and evaluation of bombesin derivatives on the basis of pan-bombesin peptides labeled with indium-111, lutetium-177, and yttrium-90 for targeting bombesin receptor-expressing tumors, Cancer Res. 64 (2004) 6707–6715.
[180] C.J. Smith, G.L. Sieckman, N.K. Owen, D.L. Hayes, D. Mazuru, W.A. Volkert, T.J. Hoffman, Radiochemical investigations of Re-188(H2O)(CO)(3)-diaminopropionic acid-SSS-bombesin(7-14)NH2 : syntheses, radiolabeling and in vitro/In vivo GRP receptor targeting studies, Anticancer Res. 23 (2003) 63–70.
[181] L.Y. Cui, Z.F. Liu, X.N. Jin, B. Jia, F. Li, F. Wang, Evaluation of Re-188-MAG(2)-RGD-bombesin for potential prostate cancer therapy, Nucl. Med. Biol. 40 (2013) 182–189.
[182] T.S. Reynolds, R.P. Bandari, Z.R. Jiang, C.J. Smith, Lutetium-177 labeled bombesin peptides for radionuclide therapy, Curr. Radiopharm. 9 (2016) 33–43.
[183] T.W. Moody, D.N. Carney, F. Cuttitta, K. Quattrocchi, J.D. Minna, High-affinity receptors for bombesin grp-like peptides on human small cell lung-cancer, Life Sci. 37 (1985) 105–113.
[184] T.W. Moody, C.B. Pert, J. Rivier, M.R. Brown, Bombesin - specific binding to rat-brain membranes, Proc. Natl. Acad. Sci. U. S. A 75 (1978) 5372–5376.
[185] J.L. Scemama, A. Zahidi, D. Fourmy, P. Fagotrevurat, N. Vaysse, L. Pradayrol, A. Ribet, Interaction of I-125 tyr4-bombesin with specific receptors on normal human pancreatic membranes, Regul. Pept. 13 (1986) 125–132.
[186] I. Avis, M. Jett, P.G. Kasprzyk, F. Cuttitta, A.M. Treston, R. Maneckjee, J.L. Mulshine, Effect of gastrin-releasing peptide on the pancreatic tumor-cell line (capan), Mol. Carcinog. 8 (1993) 214–220.
[187] H. Reile, P.E. Armatis, A.V. Schally, Characterization of high-affinity receptors for bombesin/gastrin releasing peptide on the human prostate-cancer cell-lines pc-3 and du-145 - internalization of receptor-bound (125)I-(Tyr(4)) bombesin by tumor-cells, Prostate 25 (1994) 29–38.
[188] N. Chanda, V. Kattumuri, R. Shukla, A. Zambre, K. Katti, A. Upendran, R.R. Kulkarni, P. Kan, G.M. Fent, S.W. Casteel, C.J. Smith, E. Boote, J.D. Robertson, C. Cutler, J.R. Lever, K.V. Katti, R. Kannan, Bombesin functionalized gold nanoparticles show in vitro and in vivo cancer receptor specificity, Proc. Natl. Acad. Sci. U. S. A 107 (2010) 8760–8765.
[189] F. Silva, A. Zambre, M.P.C. Campello, L. Gano, I. Santos, A.M. Ferraria, M.J. Ferreira, A. Singh, A. Upendran, A. Paulo, R. Kannan, Interrogating the role of receptor-mediated mechanisms: biological fate of peptide-functionalized radiolabeled gold nanoparticles in tumor mice, Bioconjug. Chem. 27 (2016) 1153–1164.
[190] S.A. Mantey, H.C. Weber, E. Sainz, M. Akeson, R.R. Ryan, T.K. Pradhan, R.P. Searles, E.R. Spindel, J.F. Battey, D.H. Coy, R.T. Jensen, Discovery of a high affinity radioligand for the human orphan receptor, bombesin receptor subtype 3, which demonstrates that it has a unique pharmacology compared with other mammalian bombesin receptors, J. Biol. Chem. 272 (1997) 26062–26071.
[191] T.K. Pradhan, T. Katsuno, J.E. Taylor, S.H. Kim, R.R. Ryan, S.A. Mantey, P.J. Donohue, H.C. Weber, E. Sainz, J.F. Battey, D.H. Coy, R.T. Jensen, Identification of a unique ligand which has high affinity for all four bombesin receptor subtypes, Eur. J. Pharmacol. 343 (1998) 275–287.
[192] J.C. Reubi, S. Wenger, J. Schmuckli-Maurer, J.C. Schaer, M. Gugger, Bombesin receptor subtypes in human cancers: detection with the universal radioligand I-125- D-TYR6, beta-ALA(11), PHE13, NLE14 bombesin(6-14), Clin. Cancer Res. 8 (2002) 1139–1146.
[193] B.E. Rogers, M.E. Rosenfield, M.B. Khazaeli, G. Mikheeva, M.A. Stackhouse, T.P. Liu, D.T. Curiel, D.J. Buchsbaum, Localization of iodine-125-mIP-Des-Met(14) bombesin (7-13)NH2 in ovarian carcinoma induced to express the gastrin releasing peptide receptor by adenoviral vector-mediated gene transfer, J. Nucl. Med. 38 (1997) 1221–1229.
[194] A. Zlotnik, O. Yoshie, The chemokine superfamily revisited, Immunity 36 (2012) 705–716.
[195] A. Zlotnik, O. Yoshie, Chemokines: a new classification system and their role in immunity, Immunity 12 (2000) 121–127.
[196] M. Schottelius, H.J. Wester, Molecular imaging targeting peptide receptors, Methods 48 (2009) 161–177.
[197] R.S. Taichman, C. Cooper, E.T. Keller, K.J. Pienta, N.S. Taichman, L.K. McCauley, Use of the stromal cell-derived factor-1/CXCR4 pathway in prostate cancer metastasis to bone, Cancer Res. 62 (2002) 1832–1837.
[198] A. Muller, B. Homey, H. Soto, N.F. Ge, D. Catron, M.E. Buchanan, T. McClanahan, E. Murphy, W. Yuan, S.N. Wagner, J.L. Barrera, A. Mohar, E. Verastegui, A. Zlotnik, Involvement of chemokine receptors in breast cancer metastasis, Nature 410 (2001) 50–56.
[199] R.B. Maksym, M. Tarnowski, K. Grymula, J. Tarnowska, M. Wysoczynski, R. Liu, B. Czerny, J. Ratajczak, M. Kucia, M.Z. Ratajczak, The role of stromal-derived factor-1-CXCR7 axis in development and cancer, Eur. J. Pharmacol. 625 (2009) 31–40.
[200] G. Banisadr, E. Dicou, T. Berbar, W. Rostene, A. Lombet, F. Haour, Characterization and visualization of I-125 stromal cell-derived factor-1 alpha binding to CXCR4 receptors in rat brain and human neuroblastoma cells, J. Neuroimmunol. 110 (2000) 151–160.
[201] J. Kuil, T. Buckle, F.W.B. van Leeuwen, Imaging agents for the chemokine receptor 4 (CXCR4), Chem. Soc. Rev. 41 (2012) 5239–5261.
[202] Y.J. Han, D.Z. Yin, M.Q. Zheng, W. Zhou, Z.H. Lee, L. Zhan, Y.F. Ma, M.X. Wu, L.L. Shi, N. Wang, J.B. Lee, C. Wang, Z. Lee, Y.X. Wang, Synthesis and

preliminary evaluation of a novel I-125-labeled T140 analog for quantitation of CXCR4 expression, J. Radioanal. Nucl. Chem. 284 (2010) 279–286.
[203] N. Fujii, S. Oishi, K. Hiramatsu, T. Araki, S. Ueda, H. Tamamura, A. Otaka, S. Kusano, S. Terakubo, H. Nakashima, J.A. Broach, J.O. Trent, Z.X. Wang, S.C. Peiper, Molecular-size reduction of a potent CXCR4-chemokine antagonist using orthogonal combination of conformation- and sequence-based libraries, Angew. Chem. Int. Ed. 42 (2003) 3251–3253.
[204] H. Tamamura, K. Hiramatsu, S. Ueda, Z.X. Wang, S. Kusano, S. Terakubo, J.O. Trent, S.C. Peiper, N. Yamamoto, H. Nakashima, A. Otaka, N. Fujii, Stereoselective synthesis of L-Arg-L/D-3-(2-naphthyl) alanine -type (E)-alkene dipeptide isosteres and its application to the synthesis and biological evaluation of pseudopeptide analogues of the CXCR4 antagonist FC131, J. Med. Chem. 48 (2005) 380–391.
[205] H. Tamamura, Y.O. Xu, T. Hattori, X.Y. Zhang, R. Arakaki, K. Kanbara, A. Omagari, A. Otaka, T. Ibuka, N. Yamamoto, H. Nakashima, N. Fujii, A low-molecular-weight inhibitor against the chemokine receptor CXCR4: a strong anti-HIV peptide T140, Biochem. Biophys. Res. Commun. 253 (1998) 877–882.
[206] I. Dijkgraaf, O. Demmer, U. Schumacher, N. Koglin, M. Anton, W. Brandau, M. Schwaiger, H. Kessler, H. Wester, CXCR4 receptor targeting for in-vivo imaging of metastases, Eur. J. Nucl. Med. Mol. Imaging 35 (2008). S318-S318.
[207] W. HJ, K. N, S. M, K. H, L. B, D. O, M. A, Cancer Imaging and Treatment, 2011.
[208] W. HJ, K. H, D. O, D. I, Cancer Imaging and Treatment, 2010.
[209] W.H. J, K. N, S. M, K. H, L. B, D. O, M. A, D. I, Cancer Imaging and Treatment, 2007.
[210] O.P. Medina, K. Kairemo, H. Valtanen, A. Kangasniemi, S. Kaukinen, I. Ahonen, P. Permi, A. Annila, M. Sneck, J.M. Holopainen, S.L. Karonen, P.K.J. Kinnunen, E. Koivunen, Radionuclide imaging of tumor xenografts in mice using a gelatinase-targeting peptide, Anticancer Res. 25 (2005) 33–42.
[211] N. Kondo, T. Temma, Y. Shimizu, M. Ono, H. Saji, Radioiodinated peptidic imaging probes for in vivo detection of membrane type-1 matrix metalloproteinase in cancers, Biol. Pharm. Bull. 38 (2015) 1375–1382.
[212] M.M. Yu, R.F. Wang, P. Yan, C.L. Zhang, M. Liu, Y.G. Cui, Design, synthesis and iodination of an Arg-Arg-Leu peptide for potential use as an imaging agent for human prostate carcinoma, J. Label. Comp. Radiopharm. 51 (2008) 374–378.
[213] E.M. Kim, E.H. Park, S.J. Cheong, C.M. Lee, D.W. Kim, H.J. Jeong, S.T. Lim, M.H. Sohn, K. Kim, J. Chung, Characterization, biodistribution and small-animal SPECT of I-125-labeled c-Met binding peptide in mice bearing c-Met receptor tyrosine kinase-positive tumor xenografts, Nucl. Med. Biol. 36 (2009) 371–378.
[214] K. Wang, S. Purushotham, J.Y. Lee, M.H. Na, H. Park, S.J. Oh, R.W. Park, J.Y. Park, E. Lee, B.C. Cho, M.N. Song, M.C. Baek, W. Kwak, J. Yoo, A.S. Hoffman, Y.K. Oh, I.S. Kim, B.H. Lee, In vivo imaging of tumor apoptosis using histone H1-targeting peptide, J. Control. Release 148 (2010) 283–291.
[215] W. Kwak, Y.S. Ha, N. Soni, W. Lee, S.I. Park, H. Ahn, G.I. An, I.S. Kim, B.H. Lee, J. Yoo, Apoptosis imaging studies in various animal models using radioiodinated peptide, Apoptosis 20 (2015) 110–121.
[216] M. Ueda, K. Ogawa, A. Miyano, M. Ono, S. Kizaka-Kondoh, H. Saji, Development of an oxygen-sensitive degradable peptide probe for the imaging of hypoxia-inducible factor-1-active regions in tumors, Mol. Imaging Biol. 15 (2013) 713–721.
[217] E. Koivunen, W. Arap, H. Valtanen, A. Rainisalo, O.P. Medina, P. Heikkila, C. Kantor, C.G. Gahmberg, T. Salo, Y.T. Konttinen, T. Sorsa, E. Ruoslahti, R. Pasqualini, Tumor targeting with a selective gelatinase inhibitor, Nat. Biotechnol. 17 (1999) 768–774.
[218] N. Kondo, T. Temma, Y. Shimizu, H. Watanabe, K. Higano, Y. Takagi, M. Ono, H. Saji, Miniaturized antibodies for imaging membrane type-1 matrix metalloproteinase in cancers, Cancer Sci. 104 (2013) 495–501.
[219] K. Porkka, P. Laakkonen, J.A. Hoffman, M. Bernasconi, E. Ruoslahti, A fragment of the HMGN2 protein homes to the nuclei of tumor cells and tumor endothelial cells in vivo, Proc. Natl. Acad. Sci. U. S. A 99 (2002) 7444–7449.
[220] S. Christian, J. Pilch, M.E. Akerman, K. Porkka, P. Laakkonen, E. Ruoslahti, Nucleolin expressed at the cell surface is a marker of endothelial cells in angiogenic blood vessels, JCB (J. Cell Biol.) 163 (2003) 871–878.
[221] H. Ginisty, H. Sicard, B. Roger, P. Bouvet, Structure and functions of nucleolin, J. Cell Sci. 112 (1999) 761–772.
[222] W.Y. Jia, Z.Y. Yao, J.J. Zhao, Q.B. Guan, L. Gao, New perspectives of physiological and pathological functions of nucleolin (NCL), Life Sci. 186 (2017) 1–10.
[223] C.K. Brown, R.A. Modzelewski, C.S. Johnson, M.K.K. Wong, A novel approach for the identification of unique tumor vasculature binding peptides using an E-coli peptide display library, Ann. Surg. Oncol. 7 (2000) 743–749.
[224] G.E.R. Weller, M.K.K. Wong, R.A. Modzelewski, E.X. Lu, A.L. Klibanov, W.R. Wagner, F.S. Villanueva, Ultrasonic imaging of tumor angiogenesis using contrast microbubbles targeted via the tumor-binding peptide arginine-arginine-leucine, Cancer Res. 65 (2005) 533–539.
[225] W.K. You, D.M. McDonald, The hepatocyte growth factor/c-Met signaling pathway as a therapeutic target to inhibit angiogenesis, Bmb Reports 41 (2008) 833–839.
[226] J.S. Wall, T. Richey, A. Stuckey, R. Donnell, S. Macy, E.B. Martin, A. Williams, K. Higuchi, S.J. Kennel, In vivo molecular imaging of peripheral amyloidosis using heparin-binding peptides, Proc. Natl. Acad. Sci. U. S. A 108 (2011) E586–E594.
[227] J.S. Wall, A. Williams, T. Richey, A. Stuckey, Y. Huang, C. Wooliver, S. Macy, E. Heidel, N. Gupta, A. Lee, B. Rader, E.B. Martin, S.J. Kennel, A binding-site barrier affects imaging efficiency of high affinity amyloid-reactive peptide radiotracers in vivo, PLoS One 8 (2013).
[228] E.B. Martin, A. Williams, T. Richey, C. Wooliver, A. Stuckey, J.S. Foster, S.J. Kennel, J.S. Wall, Evaluation of the effect of D-amino acid incorporation into amyloid-reactive peptides, J. Transl. Med. 15 (2017).
[229] H. Macpherson, R. Silberstein, A. Pipingas, Neurocognitive effects of multivitamin supplementation on the steady state visually evoked potential (SSVEP) measure of brain activity in elderly women, Physiol. Behav. 107 (2012) 346–354.